

UNIVERSITÀ  
DEGLI STUDI  
DI PADOVA

Università degli Studi di Padova

---

DIPARTIMENTO DI MATEMATICA “TULLIO LEVI-CIVITA”

Corso di Laurea Triennale in Matematica

Phase transition to synchronization of coupled oscillators in the Kuramoto model

Relatore:  
Prof. Marco Formentin

Laureanda: Irene Lazzarin  
Matricola: 2003223

---

Anno Accademico 2022/2023

15 dicembre 2023



# Contents

<b>Introduction</b>	<b>5</b>
<b>1 Kuramoto model</b>	<b>7</b>
1.1 Background . . . . .	7
1.2 Governing equations of the model . . . . .	8
1.3 Analysis of the solutions for a large number of oscillators . . . . .	13
1.4 Continuum limit . . . . .	21
1.4.1 Stability of the incoherent state . . . . .	23
1.5 Simulations . . . . .	31
<b>2 Kuramoto model with adding noise</b>	<b>35</b>
2.1 The Sakaguchi-Kuramoto model . . . . .	35
2.1.1 Derivation of Fokker-Planck equation . . . . .	36
2.2 Stability of the incoherent state . . . . .	38
2.3 Simulations . . . . .	43
<b>Conclusions</b>	<b>48</b>
<b>A Mathematica codes</b>	<b>49</b>
<b>Bibliography</b>	<b>59</b>



# Introduction

In this thesis we are going to present the Kuramoto model. The Kuramoto model is a mathematical model, formulated by Yoshiki Kuramoto, that describes the phenomenon of collective synchronization. This phenomenon consists of a large population of coupled limit-cycle oscillators which spontaneously locks to a common frequency, even though the natural frequencies of the individual oscillators are different.

The phenomenon of synchronization, in general speaking, is one of the most captivating cooperative phenomena in nature: it manifests itself in a wide variety of fields and everyday experiences. A paradigmatic example is the synchronous flashing of fireflies. In some South Asia forests, at night, there are a lot of fireflies. Initially they flash incoherently, but shortly after the whole swarm starts flashing in unison. Another simple example, where synchronization is a fundamental point, is the concert: each member of the orchestra plays a sequence of notes that, properly combined, provoke a deep feeling in our senses. The effect can be astonishing or a fiasco simply depending on the exact moment when the sound was emitted. In physics, biology and engineering there are also many examples: arrays of lasers, microwave oscillators, superconducting Josephson junctions, crickets that chirp in unison, pancreatic beta-cells and pacemakers heart cells, epileptic seizures in the brain and many more. All of these examples have one thing in common: each of the individual oscillator units has its own preferred frequency with which oscillate. No single oscillator is “in charge” directing the rest of population. It is the collective behaviour and interaction among the population that leads to the emergence of collective oscillations that synchronize.

Since synchronization is everywhere it has attracted the interest of many scientists for centuries who wanted to understand its relevance: for example, in the case of the fireflies, synchronous flashing may facilitate the courtship between males and females, but, in other cases the role of synchronization is still under discussion. In this dissertation we analyze the phenomenon of

synchronization in the case of coupled oscillators.

This work is organized as follows:

- **Chapter 1:** In the first chapter we first introduce the Kuramoto model and its equations in general form. We introduce also the complex order parameter which is a fundamental quantity that allows us to write the model as a mean field model and it describes the synchronization behavior of the oscillators. Then we study the solutions of equations for a large number of oscillators and we pay particular attention on the incoherent solution  $r = 0$ , that is when the oscillators are not synchronized. We find out that as the coupling strength between oscillators increases, the oscillators begin to synchronize and we find the threshold value of coupling strength at which this *phase transition* occurs. Then we discuss the stability property of the incoherent solution and finally we show some theoretical results through numerical simulations. This chapter is based on an article written by Strogatz [1].
- **Chapter 2:** In the second chapter we treat the Kuramoto model in the presence of noise. We introduce the governing equations and the Fokker-Planck equation. Then, we study the stability property of the incoherent solution and we find the threshold value of coupling strength at which *phase transition* occurs when there is noise. Finally, we discuss the differences between the two models and we show them through numerical simulations.

# Chapter 1

## Kuramoto model

### 1.1 Background

In this first section of the first chapter of the thesis we are going to find out when the phenomenon of collective synchronization, described by the Kuramoto model, was first observed. Then we will get to know the first scientists who analyzed this phenomenon, their influence and the contribution they made to the model formulated by Kuramoto a few years later.

The first recorded observation of synchronous behavior was made by Christiaan Huygens in the 17th century: he was sick in bed and he had, on the wall in front of him, two pendulum clocks hanging from a common support. He made the pendulums swing at differing paces and he observed that, half an hour later,

*they always returned to synchronism and kept it constantly afterwards, as long as I let them go.*

As he wrote in a letter to his father on 25 February 1665. So the pendulum clocks always swung together and never varied. According to Huygens, this happened due to a sort of *sympathy* [2].

The phenomenon of collective synchronization in populations of coupled oscillators was studied, for the first time ever, by the American mathematician Norbert Wiener. He discovered it was a common phenomenon in the natural world and he also hypothesized that it was involved in the generation of alpha rhythms in the brain. But Wiener's approach, based on Fourier integrals, was wrong. A major breakthrough was made, in 1967, by the biologist Winfree. He formulated the problem in terms of a huge population of interacting

limit-cycle oscillators assuming the coupling weak and the oscillators nearly identical. Then Winfree supposed also that each oscillator was coupled to the collective rhythm generated by the whole population. This simplification is the basic concept of the mean-field approximation that will be a key point in our treatment of the Kuramoto model. The governing equations of Winfree model are the following:

$$\dot{\theta}_i = \omega_i + \left( \sum_{j=1}^N X(\theta_j) \right) Z(\theta_i), \quad i = 1, \dots, N,$$

where  $\theta_i$  represents the phase of oscillator  $i$  and  $\omega_i$  its natural frequency. Each oscillator  $j$  exerts a phase-dependent influence  $X(\theta_j)$  on all the others; the corresponding response of oscillator  $i$  depends on its phase  $\theta_i$ , through the sensitivity function  $Z(\theta_i)$ . Winfree found out that when the spread of natural frequencies is large compared to the coupling, the system behaves incoherently and each oscillator runs at its natural frequency. Instead, when the spread decreased, the incoherence persists until a certain threshold is crossed, then a macroscopic fraction of oscillators suddenly synchronize to a common frequency. So Winfree realized that synchronization can be understood as a “threshold process” but the model he proposed was hard to solve. The first one who formulated a mathematically tractable model about this phenomenon was Kuramoto in 1975. His model, known as *Kuramoto model* (sometime called KM), is a simplification of Winfree’s model and is based on phase oscillators running at arbitrary intrinsic frequencies and coupled through their sine of their phase differences. This model can be used to study many synchronization patterns and it can be applied in many different contexts and these are the reasons why KM is so important.

## 1.2 Governing equations of the model

In this section we are going to introduce the Kuramoto model. Before analyzing the governing equations of the model, we have to explain some notions about oscillator’s theory that will be fundamental for our treatment.

In order to describe the state of an oscillator at some instant we have to introduce two variables: the position (specified by an angle) and the velocity. These two variables give rise to the *phase space*.

**Definition 1.1** (Phase space). *A phase space is a space in which all possible “states” of a dynamical system (here a system of oscillators) are represented, with each possible state corresponding to one unique point in the phase space.*



To describe the motion of an oscillator, then, we can talk about its motion in phase space. The oscillators studied in this thesis move in phase space in a special way: when left to themselves, they eventually revisit the same points over and over. So the steady-state evolution of an oscillator corresponds to some closed curve in phase space. This closed curve is called a *limit cycle*.

**Definition 1.2** (Limit cycle). *A limit cycle is a closed trajectory in phase space having the property that at least one other trajectory spirals into it either as time approaches infinity or as time approaches negative infinity. In other words, the limit cycle is an isolated trajectory (isolated in the sense that neighboring trajectories are not closed)*

**Definition 1.3.** *The phase  $\theta$  of an oscillator is defined so that it grows uniformly in time and gains  $2\pi$  radians for each trip around the limit cycle. Each point on the cycle corresponds to a certain value of the phase.*

**Observation 1.1.** *We can note that the phase is defined to grow uniformly in time, while the system may not evolve uniformly along the limit cycle (it may go faster in phase space in some places on the cycle than others).*

**Definition 1.4.** *The natural frequency  $\omega$  of an oscillator is a quantity that characterizes how quickly the oscillator travels around its limit cycle in the absence of outside influences.*

At this stage, we can give the following definition:

**Definition 1.5** (Kuramoto model). *The Kuramoto model consists of a population of  $N$  coupled limit-cycle oscillators, having phases  $\theta_i$  and natural frequencies  $\omega_i$ , whose dynamics is governed by phase equations of the following universal form:*

$$\dot{\theta}_i = \omega_i + \sum_{j=1}^N \Gamma_{ij}(\theta_j - \theta_i), \quad i = 1, \dots, N, \quad (1.1)$$

where  $\Gamma_{ij}$  are interaction functions.

This phase model is a simplification of the formulation made by Winfree but these equations are still far too difficult to analyze because the interaction functions  $\Gamma_{ij}$  could have many Fourier harmonics and the connection topology is unspecified. In order to avoid this problem, we consider the mean-field case because it is the most tractable.

**Definition 1.6** (Mean-field theory). *In physics and probability theory, the mean-field theory studies the behavior of high-dimensional random stochastic models by studying a simpler model that approximates the original by averaging over degrees of freedom. So the overall effects of all system elements on a single element are approximated to a single average effect, thus with mean-field theory we reduce any many-body problem into an effective one-body problem.*

To transform the original model (1.1) into a mean-field model we use a sine function to couple the oscillators. Therefore, we consider equally weighted, all-to-all, purely sinusoidal coupling:

$$\Gamma_{ij}(\theta_j - \theta_i) = \frac{K}{N} \sin(\theta_j - \theta_i), \quad i, j = 1, \dots, N, \quad (1.2)$$

where  $K \geq 0$  is a constant sizing the coupling strength between oscillators and the factor  $\frac{1}{N}$  ensures that the model has a non-trivial limiting behavior as  $N \rightarrow \infty$ .

**Observation 1.2.** *If  $K = 0$  we obtain a simple set of “phases”,  $\theta_i = \theta_i(t)$ ,  $i = 1, \dots, N$ , which evolves as*

$$\dot{\theta}_i(t) = \omega_i t + \theta_i(0).$$

*Hence, when there is no coupling between the oscillators each oscillator rotates at its own frequency and has its own phase. Thus, the phases and the frequencies of the oscillators are incoherent.*

With the choice (1.2), the system of equations (1.1) become:

$$\dot{\theta}_i = \omega_i + \frac{K}{N} \sum_{j=1}^N \sin(\theta_j - \theta_i), \quad i = 1, \dots, N. \quad (1.3)$$

The natural frequencies  $\omega_i$  are distributed according to some probability density  $g(\omega)$ . In order to simplify the analysis, we assume that  $g(\omega)$  is unimodal and symmetric about its mean frequency  $\Omega$ . We give the following definitions:

**Definition 1.7.** *A unimodal probability distribution is a probability distribution which has a single peak. Unimodality means that a single value in the distribution occurs more frequently than any other value. The peak represents the most common value, also known as the mode.*

**Definition 1.8.** *The probability density  $g(\omega)$  is called “symmetric” about its mean frequency  $\Omega$  if  $g(\Omega + \omega) = g(\Omega - \omega)$  for all  $\omega$ .*

**Definition 1.9.** *In a symmetric unimodal distribution, mean, median, and mode all occur at the peak.*

**Example.** *The most common example of unimodal and symmetric distribution is the Normal distribution.*

Thanks to these properties of  $g(\omega)$ , we can set the mean frequency  $\Omega = 0$  by applying the transformation  $\theta_i \rightarrow \theta_i + \Omega t$  for all  $i$ , which physically means moving into a rotating frame at frequency  $\Omega$ . In this way, the governing equations (1.3) are invariant and the mean of  $g(\omega)$  is shifted to zero so the natural frequencies have zero mean. So henceforth,  $g(\omega) = g(-\omega)$  for all the  $\omega$  and the  $\omega_i$  represent deviations from the mean frequency  $\Omega$ . We also suppose that  $g(\omega)$  is nowhere increasing on  $[0, \infty)$ , i.e.,  $g(\omega) \geq g(v)$  whenever  $\omega \leq v$ .

We want to write Eq. (1.3) in a more convenient form to visualize the dynamics of the phases. To this end, we introduce the complex order parameter.

**Definition 1.10** (Complex order parameter). *The complex order parameter is the macroscopic quantity*

$$r e^{i\psi} = \frac{1}{N} \sum_{j=1}^N e^{i\theta_j}, \quad (1.4)$$

which is an “object” that can be seen as the collective rhythm produced by the entire population of oscillators. It represents the centroid of the phases. The radius  $r(t)$ , with  $0 \leq r(t) \leq 1$ , measures the coherence of the oscillator population and  $\psi(t)$  the average phase of all oscillators.

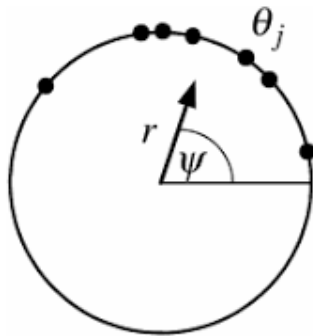
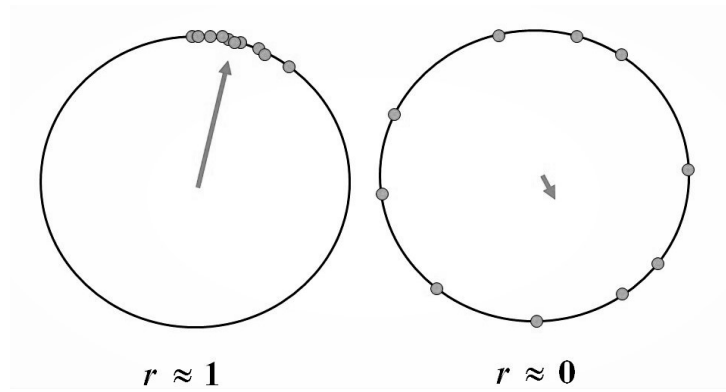


Figure 1.1: Geometric interpretation of order parameter.

The complex order parameter can be represented in this way, as we can see in the figure 1.1: the phases  $\theta_j$  are plotted on the unit circle in the complex plane, their centroid is given by the complex number  $re^{i\psi}$ , shown as an arrow. There are two relevant situations, as we can see in the figure 1.2 taken from [3] : the case in which  $r \approx 1$  that means that all the oscillators move in a single tight clump so the population acts like a giant single oscillator and the opposite case, where  $r \approx 0$ , that means the individual oscillators are scattered around the circle, so they run independently, incoherently, and no macroscopic rhythm is produced.

Figure 1.2



After we introduced the order parameter, the system of equations (1.3) can be rewritten in this way: we multiply both sides of (1.4) by  $e^{-i\theta_i}$ ,

$$re^{i\psi}e^{-i\theta_i} = \frac{1}{N} \sum_{j=1}^N e^{i\theta_j}e^{-i\theta_i},$$

for the law of exponents,

$$re^{i(\psi-\theta_i)} = \frac{1}{N} \sum_{j=1}^N e^{i(\theta_j-\theta_i)}. \quad (1.5)$$

Applying Euler's Formula,  $e^{ix} = \cos(x) + i \sin(x)$ , we obtain

$$r(\cos(\psi - \theta_i) + i \sin(\psi - \theta_i)) = \frac{1}{N} \sum_{j=1}^N (\cos(\theta_j - \theta_i) + i \sin(\theta_j - \theta_i)).$$

Then, equating imaginary parts and simplifying  $i$  on both sides, we have

$$r \sin(\psi - \theta_i) = \frac{1}{N} \sum_{j=1}^N \sin(\theta_j - \theta_i).$$

So the governing equations (1.3) become

$$\dot{\theta}_i = \omega_i + Kr \sin(\psi - \theta_i), \quad i = 1, \dots, N.$$

**Definition 1.11.** *The governing equations of the Kuramoto model as a mean field model are*

$$\dot{\theta}_i = \omega_i + Kr \sin(\psi - \theta_i), \quad i = 1, \dots, N. \quad (1.6)$$

**Observation 1.3.** *The system of equations (1.6) describes the system as a mean field model: each oscillator appears to run independently from all the others but obviously they are interacting, in fact each oscillator is coupled to the common average phase  $\psi(t)$  with coupling strength given by  $Kr$ . The phase  $\theta_i$  is pulled toward the mean phase  $\psi$  and not toward the phase of any individual oscillator as at the beginning.*

**Observation 1.4.** *There is a proportionality between the effective strength of the coupling and the coherence  $r$ : if the population of oscillators becomes more coherent, the radius  $r$  grows (it is getting closer and closer to 1) and so  $Kr$  increases. When the effective coupling boosts, more oscillators join the synchronized group. This link between  $K$  and  $r$  is very clear in the figure 1.5 in the last section of the chapter.*

### 1.3 Analysis of the solutions for a large number of oscillators

In this section we analyze the long-term behavior of the solutions in the limit  $N \rightarrow \infty$ . We focus the study on the research of steady solutions.

**Definition 1.12.** *In a steady solution the radius  $r(t)$  is constant (so all the oscillators are independent) and  $\psi(t)$  rotates uniformly at the mean frequency  $\Omega$ .*

Choosing the origin of the rotating frame correctly, we can set  $\psi \equiv 0$  without loss of generality. Considering this assumption, we have

$$\begin{aligned} \dot{\theta}_i &= \omega_i + Kr \sin(\psi - \theta_i) \\ &= \omega_i + Kr \sin(-\theta_i) \\ &= \omega_i - Kr \sin(\theta_i), \end{aligned} \quad (1.7)$$

for  $i = 1, \dots, N$ .

After writing governing equations into a new form, we consider the *self-consistency* condition: we want to solve for the resulting motions of all the oscillators which depend on  $r$  as a parameter but these motions in turn imply values for  $r$  and  $\psi$  which must be consistent with the original values that had been assumed.

**Proposition 1.1.** *The solutions of (1.7) show that there are two types of long-term behavior, depending on the size of  $|\omega_i|$  relative to  $Kr$ :*

- *if  $|\omega_i| \leq Kr$  there are two stationary points: one of these is a stable fixed point defined implicitly by*

$$\omega_i = Kr \sin(\theta_i),$$

*where  $|\theta_i| \leq \frac{\pi}{2}$ .*

- *if  $|\omega_i| > Kr$ , the oscillators will rotate, since  $|\dot{\theta}_i| \neq 0$ .*

**Definition 1.13** (Locked oscillators). *The oscillators characterized by  $|\omega_i| \leq Kr$  are called “locked” because they are phase-locked at frequency  $\Omega$  in the original frame.*

**Definition 1.14** (Drifting oscillators). *The oscillators characterized by  $|\omega_i| > Kr$  are called “drifting” exactly because they run around the circle in a nonuniform manner, accelerating near some phases and hesitating at others.*

Therefore, the population can be divided into two groups: *locked* and *drifting* oscillators, the first one correspond to the center of  $g(\omega)$  and the second one to the tails. The existence of the drifting oscillators would seem to contradict that  $r$  and  $\psi$  are constant because of the buzz around the circle so it's weird that the centroid of the population remain constant but we can avoid this problem by demanding that the drifting oscillators form a stationary distribution on the circle. In this way the centroid remains fixed although the individual oscillators continue to move.

**Definition 1.15.** *The stationary density of drifting oscillators is*

$$\rho(\theta, \omega) = \frac{C}{|\omega - Kr \sin(\theta)|}. \quad (1.8)$$

*This density has the following properties:*

- is inversely proportional to the speed at  $\theta$ , as expected: oscillators pile up at slow places and thin out at fast places on the circle.
- the normalization constant  $C$  is

$$C = \frac{\sqrt{\omega^2 - (Kr)^2}}{2\pi},$$

determined by  $\int_{-\pi}^{\pi} \rho(\theta, \omega) d\theta = 1$  for each  $\omega$ .

After these considerations, we can give the following definition:

**Definition 1.16** (Self-consistency condition). *The self-consistency condition of the complex order parameter is*

$$\langle e^{i\theta} \rangle = \langle e^{i\theta} \rangle_{lock} + \langle e^{i\theta} \rangle_{drift}$$

where  $\langle e^{i\theta} \rangle = re^{i\psi}$  (so the angular brackets denote population averages).

Since  $\psi = 0$ , the self-consistency equation will reduce to

$$r = \langle e^{i\theta} \rangle_{lock} + \langle e^{i\theta} \rangle_{drift},$$

because  $\langle e^{i\theta} \rangle = re^{i\psi} = r$ . The first term on the right hand side can be rewritten in this way, using Euler's Formula and linearity property of mean,

$$\langle e^{i\theta} \rangle_{lock} = \langle \cos \theta + i \sin \theta \rangle_{lock} = \langle \cos \theta \rangle_{lock} + i \langle \sin \theta \rangle_{lock}. \quad (1.9)$$

As regards the imaginary part of (1.9), we show the following Proposition:

**Proposition 1.2.** *We have  $\langle \sin \theta \rangle_{lock} = 0$ .*

*Proof.* As we stated at the beginning,  $g(\omega) = g(-\omega)$ , thus the distribution of locked phases is symmetric about  $\theta = 0$ . Therefore, we have

$$\begin{aligned} \langle \sin \theta \rangle_{lock} &= \int_{-Kr}^{Kr} \sin \theta(\omega) g(\omega) d\omega \\ &= \int_{-Kr}^0 \sin \theta(\omega) g(\omega) d\omega + \int_0^{Kr} \sin \theta(\omega) g(\omega) d\omega \\ &= - \int_{Kr}^0 \sin \theta(-\omega) g(-\omega) d\omega + \int_0^{Kr} \sin \theta(\omega) g(\omega) d\omega \\ &= - \int_{Kr}^0 \sin \theta(-\omega) g(\omega) d\omega + \int_0^{Kr} \sin \theta(\omega) g(\omega) d\omega \\ &= \int_{Kr}^0 \sin \theta(\omega) g(\omega) d\omega + \int_0^{Kr} \sin \theta(\omega) g(\omega) d\omega \\ &= - \int_0^{Kr} \sin \theta(\omega) g(\omega) d\omega + \int_0^{Kr} \sin \theta(\omega) g(\omega) d\omega \\ &= 0 \end{aligned}$$

□

However, as regards the real part of (1.9), we have the following result:

**Proposition 1.3.** *We have*

$$\langle \cos \theta \rangle_{lock} = Kr \int_{-\frac{\pi}{2}}^{\frac{\pi}{2}} \cos^2 \theta g(Kr \sin \theta) d\theta.$$

*Proof.* We have

$$\langle \cos \theta \rangle_{lock} = \int_{-Kr}^{Kr} \cos \theta(\omega) g(\omega) d\omega.$$

If we apply the variable change  $\omega = Kr \sin \theta$  we obtain,

$$\begin{aligned} \langle \cos \theta \rangle_{lock} &= \int_{-\frac{\pi}{2}}^{\frac{\pi}{2}} \cos \theta g(Kr \sin \theta) d(Kr \sin \theta) \\ &= \int_{-\frac{\pi}{2}}^{\frac{\pi}{2}} \cos \theta g(Kr \sin \theta) Kr \cos \theta d\theta \\ &= Kr \int_{-\frac{\pi}{2}}^{\frac{\pi}{2}} \cos^2 \theta g(Kr \sin \theta) d\theta. \end{aligned}$$

□

Therefore, Eq. (1.9) becomes

$$\langle e^{i\theta} \rangle_{lock} = Kr \int_{-\frac{\pi}{2}}^{\frac{\pi}{2}} \cos^2 \theta g(Kr \sin \theta) d\theta.$$

Now we consider the drifting oscillators and we prove the following result:

**Proposition 1.4.** *The drifting oscillators don't contribute to the order parameter, that is*

$$\langle e^{i\theta} \rangle_{drift} = 0.$$

*Proof.* We have

$$\langle e^{i\theta} \rangle_{drift} = \int_{-\pi}^{\pi} \int_{|\omega| > Kr} e^{i\theta} \rho(\theta, \omega) g(\omega) d\omega d\theta$$

and we have to prove that this integral vanishes. We proceed in this way.

$$\begin{aligned} \langle e^{i\theta} \rangle_{drift} &= \int_{-\pi}^{\pi} \int_{-\infty}^{-Kr} e^{i\theta} \rho(\theta, \omega) g(\omega) d\omega d\theta \\ &\quad + \int_{-\pi}^{\pi} \int_{Kr}^{\infty} e^{i\theta} \rho(\theta, \omega) g(\omega) d\omega d\theta. \end{aligned} \tag{1.10}$$



Making the variable change  $\omega \rightarrow -\omega$  to the first term of (1.10) gives

$$\begin{aligned} \langle e^{i\theta} \rangle_{drift} = & - \int_{-\pi}^{\pi} \int_{\infty}^{Kr} e^{i\theta} \rho(\theta, -\omega) g(-\omega) d\omega d\theta \\ & + \int_{-\pi}^{\pi} \int_{Kr}^{\infty} e^{i\theta} \rho(\theta, \omega) g(\omega) d\omega d\theta. \end{aligned} \quad (1.11)$$

Making a further change of variable  $\theta \rightarrow \theta + \pi$  to the first integral of (1.11) and noting the periodicity of the first term, gives

$$\begin{aligned} \langle e^{i\theta} \rangle_{drift} = & - \int_{-\pi}^{\pi} \int_{\infty}^{Kr} e^{i(\theta+\pi)} \rho(\theta + \pi, -\omega) g(-\omega) d\omega d\theta \\ & + \int_{-\pi}^{\pi} \int_{Kr}^{\infty} e^{i\theta} \rho(\theta, \omega) g(\omega) d\omega d\theta. \end{aligned} \quad (1.12)$$

Now we change the order of the  $\omega$  integration and we can note that  $e^{i\pi} = \cos \pi + i \sin \pi = -1$ , so we get

$$\begin{aligned} \langle e^{i\theta} \rangle_{drift} = & - \int_{-\pi}^{\pi} \int_{Kr}^{\infty} e^{i\theta} \rho(\theta + \pi, -\omega) g(-\omega) d\omega d\theta \\ & + \int_{-\pi}^{\pi} \int_{Kr}^{\infty} e^{i\theta} \rho(\theta, \omega) g(\omega) d\omega d\theta. \end{aligned} \quad (1.13)$$

From our initial assumption on the distribution,  $g(\omega) = g(-\omega)$ , and, from equation (1.8), it seen that  $\rho(\theta + \pi, -\omega) = \rho(\theta, \omega)$ . Therefore,

$$\langle e^{i\theta} \rangle_{drift} = 0,$$

consequently the drifting oscillators don't contribute to the order parameter.  $\square$

Thus, the self-consistency condition reduces to

$$r = Kr \int_{-\frac{\pi}{2}}^{\frac{\pi}{2}} \cos^2 \theta g(Kr \sin \theta) d\theta. \quad (1.14)$$

This equation has always the trivial solution,  $r = 0$ , for any value of the coupling constant  $K$ . For  $r = 0$  we can note, from (1.8), that  $\rho(\theta, \omega) = \frac{1}{2\pi}$  for all values of  $\theta$  and  $\omega$ , meaning that there is an equal probability of finding an oscillator's phase anywhere on the circle.

**Definition 1.17** (Incoherent solution). *The solution  $r = 0$  is called incoherent solution because the oscillators run incoherently.*

**Definition 1.18** (Incoherent state). *The state  $\rho(\theta, \omega) = \frac{1}{2\pi}$  is called incoherent state.*

However Eq. (1.14) also has a second branch of solutions, corresponding to  $0 < r \leq 1$ , that describes the *partially synchronized* phase, satisfying

$$1 = K \int_{-\frac{\pi}{2}}^{\frac{\pi}{2}} \cos^2 \theta g(Kr \sin \theta) d\theta. \quad (1.15)$$

This branch bifurcates continuously from  $r = 0$  at the value  $K = K_c$ . This value represents the point at which the *phase transition* occurs: for  $K < K_c$  the oscillators run incoherently (because  $r = 0$ ), from  $K = K_c$  the oscillators begin to synchronize.

Now, we can prove the following key result:

**Theorem 1.1.** *The threshold value at which the second branch of solutions bifurcates from the first is*

$$K_c = \frac{2}{\pi g(0)}.$$

*Proof.* Letting  $r \rightarrow 0^+$  in (1.15) we have

$$1 = K \int_{-\frac{\pi}{2}}^{\frac{\pi}{2}} \cos^2 \theta g(0) d\theta.$$

For the double-angle formula of cosine we have

$$\cos 2\theta = \cos^2 \theta - \sin^2 \theta = 2 \cos^2 \theta - 1.$$

Substituting  $\cos^2 \theta = \frac{\cos 2\theta + 1}{2}$  into the integral we obtain

$$\begin{aligned} 1 &= K \int_{-\frac{\pi}{2}}^{\frac{\pi}{2}} \frac{\cos 2\theta + 1}{2} g(0) d\theta \\ 1 &= \frac{Kg(0)}{2} \int_{-\frac{\pi}{2}}^{\frac{\pi}{2}} (\cos 2\theta + 1) d\theta \\ 1 &= \frac{Kg(0)}{2} \left[ \frac{\sin 2\theta}{2} + \theta \right]_{-\frac{\pi}{2}}^{\frac{\pi}{2}} \\ 1 &= \frac{Kg(0)}{2} \pi. \end{aligned}$$

□

**Observation 1.5.** *We can note that the threshold value depends only on which distribution  $g$  we are considering.*

It is interesting at this stage to see how the growth of  $r$ , at the critical point, scales with increasing  $K$ . We show the following Theorem:

**Theorem 1.2.** *Near onset, the amplitude of the bifurcating branch obeys the square-root scaling law:*

$$r \approx \sqrt{\frac{16}{\pi K_c^3}} \sqrt{\frac{\mu}{-g''(0)}},$$

where

$$\mu = \frac{K - K_c}{K_c}$$

is the normalized distance above threshold.

*Proof.* To prove this result we can Taylor expand  $g$  in (1.15) around  $r = 0$ . We have,

$$1 = K \int_{-\frac{\pi}{2}}^{\frac{\pi}{2}} \left[ g(0) + g'(0)Kr \sin(\theta) + \frac{g''(0)}{2}K^2r^2 \sin^2(\theta) \right] \cos^2 \theta d\theta + O(r^3).$$

Assuming that  $g(\omega)$  has a maximum value at  $\omega = 0$ , we have  $g'(0) = 0$ . Integrating, we find

$$1 = K \left[ g(0) \frac{\pi}{2} + \frac{1}{16} \pi K^2 r^2 g''(0) \right] + O(r^3) = \frac{K}{K_c} + \frac{1}{16} \pi K^3 r^2 g''(0) + O(r^3).$$

Thus, we obtain

$$r \approx \frac{4}{K_c^2} \sqrt{\frac{K - K_c}{\pi g''(0)}}. \quad (1.16)$$

We can rewritten (1.16) in the following form

$$r \approx \sqrt{\frac{16}{\pi K_c^3}} \sqrt{\frac{\mu}{-g''(0)}},$$

to point out  $\mu = \frac{K - K_c}{K_c}$ . □

**Observation 1.6.** *We can see that the bifurcation is supercritical if  $g''(0) < 0$  and it is subcritical if  $g''(0) > 0$ .*

**Example** (Lorentzian density). *If we consider the special case of a Lorentzian density*

$$g(\omega) = \frac{\gamma}{\pi(\gamma^2 + \omega^2)},$$

where  $\gamma$  is the distribution width, we can obtain an explicit value for  $r$ . Substituting the density into Eq. (1.15) we have

$$1 = \frac{K\gamma}{\pi} \int_{-\frac{\pi}{2}}^{\frac{\pi}{2}} \frac{1}{\gamma^2 + K^2 r^2 \sin^2(\theta)} \cos^2(\theta) d\theta. \quad (1.17)$$

Integrating Eq. (1.17), we obtain

$$1 = \frac{\gamma - \sqrt{K^2 r^2 + \gamma^2}}{K r^2}. \quad (1.18)$$

For the Lorentzian density,  $K_c = \frac{2}{\pi g(0)} = 2\gamma$ . If we solve Eq. (1.18) for  $r$  we find

$$r = \sqrt{1 - \frac{K_c}{K}}$$

for all  $K \geq K_c$ .

The figure below illustrates the bifurcation diagram for the Kuramoto model.

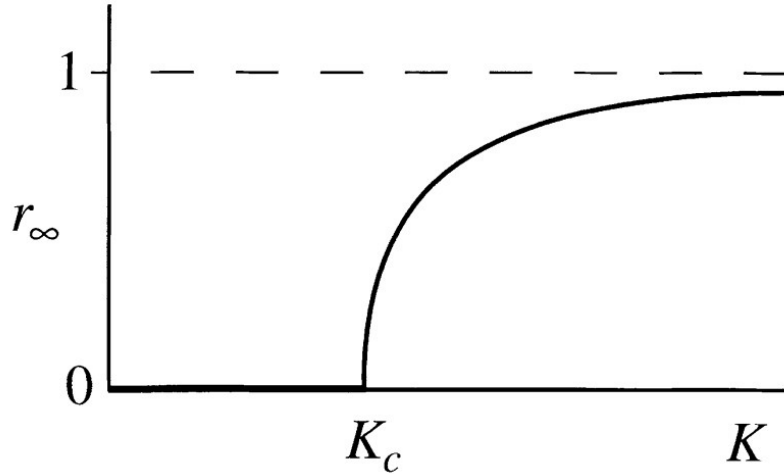


Figure 1.3: Theoretical curve: for  $K < K_c$  we have  $r = 0$  that means that the oscillators run independently, at  $K = K_c$  the phase transition occurs and the oscillators begin to synchronize.

## 1.4 Continuum limit

In this section we want to focus on the problem of the stability of the steady solutions. Kuramoto's original construction of incoherent and partially synchronized phases concerns purely stationary states. Moreover, he did not establish any of their stability properties. The linear stability theory of incoherence was published by Strogatz. To study the stability it is better to work with the probability density  $\rho(\theta, t, \omega)$ . So, at this point, we assume an infinite continuum of oscillators spread over the unit circle for each natural frequency  $\omega$ . We introduce the density function  $\rho(\theta, t, \omega)$ , where  $\rho(\theta, t, \omega)d\theta$  represents the part of the oscillators with natural frequency  $\omega$  whose phase lies between  $\theta$  and  $\theta + d\theta$  at the time  $t$ .

**Observation 1.7.** *We can see that  $\rho$  is non-negative,  $2\pi$ -periodic in  $\theta$ , i.e.  $\rho(\theta + 2\pi, t, \omega) = \rho(\theta, t, \omega)$ , and satisfies the normalization*

$$\int_0^{2\pi} \rho(\theta, t, \omega) d\theta = 1$$

for all  $t$  and  $\omega$ .

At this point, we introduce these definitions:

**Definition 1.19.** *The density satisfies the “continuity equation”*

$$\frac{\partial \rho}{\partial t} = -\frac{\partial}{\partial \theta}(\rho v) \quad (1.19)$$

that expresses the conservation of oscillators of frequency  $\omega$  and describes the evolution of  $\rho$  over the time.

**Definition 1.20.** *The velocity  $v(\theta, t, \omega)$  in eq. (1.19) is the instantaneous velocity of an oscillator at position  $\theta$  and its expression, obtaining from (1.6), is the following,*

$$v(\theta, t, \omega) = \omega + Kr \sin(\psi - \theta). \quad (1.20)$$

Since we are considering an infinite continuum of oscillators we have to re-define the complex order parameter (1.4) in a new way.

**Definition 1.21.** *The complex order parameter in case of infinite oscillators is*

$$r e^{i\psi} = \int_0^{2\pi} \int_{-\infty}^{\infty} e^{i\theta} \rho(\theta, t, \omega) g(\omega) d\omega d\theta. \quad (1.21)$$

**Observation 1.8.** *Eq. (1.21) is obtained by applying the law of large numbers to (1.4).*

At this point we are ready to enounce the following Theorem:

**Theorem 1.3** (Continuum limit). *The continuum limit of the Kuramoto model is the nonlinear partial integro-differential equation*

$$\frac{\partial \rho}{\partial t} = -\frac{\partial}{\partial \theta} \left[ \rho \left( \omega + K \int_0^{2\pi} \int_{-\infty}^{\infty} \sin(\theta' - \theta) \rho(\theta', t, \omega') g(\omega') d\omega' d\theta' \right) \right]. \quad (1.22)$$

*Proof.* We know that the instantaneous velocity of an oscillator is given by

$$\begin{aligned} v(\theta, t, \omega) &= \omega + Kr \sin(\psi - \theta) \\ &= \omega + Kr(\sin \psi \cos \theta - \cos \psi \sin \theta). \end{aligned} \quad (1.23)$$

Substituting Eq. (1.23) into Eq. (1.19), we find

$$\frac{\partial \rho}{\partial t} = -\frac{\partial}{\partial \theta} [\rho[\omega + Kr(\sin \psi \cos \theta - \cos \psi \sin \theta)]]. \quad (1.24)$$

Now, we consider the complex order parameter

$$r e^{i\psi} = \int_0^{2\pi} \int_{-\infty}^{\infty} e^{i\theta'} \rho(\theta', t, \omega') g(\omega') d\omega' d\theta',$$

that can be rewritten in this way, using Euler's Formula,

$$r(\cos \psi + i \sin \psi) = \int_0^{2\pi} \int_{-\infty}^{\infty} (\cos \theta' + i \sin \theta') \rho(\theta', t, \omega') g(\omega') d\omega' d\theta'.$$

Then, we have

$$r \cos \psi = \int_0^{2\pi} \int_{-\infty}^{\infty} \cos \theta' \rho(\theta', t, \omega') g(\omega') d\omega' d\theta', \quad (1.25)$$

$$r \sin \psi = \int_0^{2\pi} \int_{-\infty}^{\infty} \sin \theta' \rho(\theta', t, \omega') g(\omega') d\omega' d\theta'. \quad (1.26)$$

We substitute Eq. (1.25) and Eq. (1.26) into Eq. (1.24). We obtain

$$\begin{aligned} \frac{\partial \rho}{\partial t} &= -\frac{\partial}{\partial \theta} \left[ \rho \left( \omega + K \cos \theta \int_0^{2\pi} \int_{-\infty}^{\infty} \sin \theta' \rho(\theta', t, \omega') g(\omega') d\omega' d\theta' \right. \right. \\ &\quad \left. \left. - K \sin \theta \int_0^{2\pi} \int_{-\infty}^{\infty} \cos \theta' \rho(\theta', t, \omega') g(\omega') d\omega' d\theta' \right) \right], \end{aligned}$$

which is equivalent to

$$\frac{\partial \rho}{\partial t} = -\frac{\partial}{\partial \theta} \left[ \rho \left( \omega + K \int_0^{2\pi} \int_{-\infty}^{\infty} \sin(\theta' - \theta) \rho(\theta', t, \omega') g(\omega') d\omega' d\theta' \right) \right].$$

□

**Observation 1.9.** We can note that the stationary states of (1.22) are exactly the steady solutions found before. In fact, if we set  $\frac{\partial \rho}{\partial t} = 0$ , we find  $\rho v = C(\omega)$ , where  $C(\omega)$  is a  $\omega$ -dependent constant. If  $C(\omega) \neq 0$  we obtain the stationary density (1.8) for the drifting oscillators. If  $C(\omega) = 0$ , we find that  $\rho$  is a delta function in  $\theta$ , based at the locked phase.

**Definition 1.22.** In mathematical physics, the Dirac delta distribution is a generalized function or distribution over the real numbers, whose value is zero everywhere except at zero, and whose integral over the entire real line is equal to one.

It is convenient to consider as the stationary state the *incoherent state*,  $\rho_0(\theta, \omega) \equiv \frac{1}{2\pi}$ .

### 1.4.1 Stability of the incoherent state

Now, let's deal with the linearity stability problem of the incoherent state. In order to solve the stability issue, we define

$$\rho(\theta, t, \omega) = \frac{1}{2\pi} + \epsilon \eta(\theta, t, \omega), \quad (1.27)$$

where  $\epsilon \ll 1$  and  $\eta$  is the perturbation which has zero mean. We write  $\eta$  as a Fourier series in  $\theta$ :

$$\eta(\theta, t, \omega) = c(t, \omega)e^{i\theta} + c^*(t, \omega)e^{-i\theta} + \eta^\perp(\theta, t, \omega).$$

In this equation  $c = c_1$  is the first Fourier coefficient,  $c^* = c_1^*$  is its complex conjugate and  $\eta^\perp$  contains all the higher harmonics of  $\eta$ . Since  $\eta$  is real we have  $c_{-1} = c_1^*$ . We write the perturbation in this form because the linearized amplitude equation for the first harmonic,  $c(t, \omega)$ , is the only with nontrivial dynamics [4]. The reason is the sinusoidal coupling of the Kuramoto model as we prove in the following Proposition.

**Proposition 1.5.** *The expression for  $r$  depends only on the first harmonic.*

*Proof.* We substitute (1.27) into (1.21) obtaining

$$r e^{i\psi} = \int_0^{2\pi} \int_{-\infty}^{\infty} e^{i\theta} \left[ \frac{1}{2\pi} + \epsilon \eta \right] g(\omega) d\omega d\theta, \quad (1.28)$$

which can be simplified by noting that the term  $\frac{e^{i\theta}}{2\pi}$  will integrate to zero under the  $\theta$  integral. Thus, we have

$$r e^{i\psi} = \epsilon \int_0^{2\pi} \int_{-\infty}^{\infty} e^{i\theta} \eta(\theta, t, \omega) g(\omega) d\omega d\theta.$$

Now we define  $r = r_1 \epsilon$ , obtaining

$$r_1 e^{i\psi} = \int_0^{2\pi} \int_{-\infty}^{\infty} e^{i\theta} \eta(\theta, t, \omega) g(\omega) d\omega d\theta.$$

At this point, we substitute the Fourier series,

$$\begin{aligned} r_1 e^{i\psi} &= \int_0^{2\pi} \int_{-\infty}^{\infty} e^{i\theta} \left( \sum_{n=-\infty}^{\infty} c_n(t, \omega) e^{in\theta} \right) g(\omega) d\omega d\theta \\ &= \int_{-\infty}^{\infty} \sum_{n=-\infty}^{\infty} c_n(t, \omega) \left( \int_0^{2\pi} e^{i(n+1)\theta} d\theta \right) g(\omega) d\omega \\ &= \int_{-\infty}^{\infty} \sum_{n=-\infty}^{\infty} c_n(t, \omega) 2\pi \delta_{n,-1} g(\omega) d\omega \\ &= 2\pi \int_{-\infty}^{\infty} c_{-1}(t, \omega) g(\omega) d\omega \\ &= 2\pi \int_{-\infty}^{\infty} c^*(t, \omega) g(\omega) d\omega. \end{aligned}$$

From this equation we find out that we can solve for  $r(t)$  if we know only the first harmonic of  $\eta$ .

□

Now we substitute (1.27) into (1.19) obtaining

$$\frac{\partial c}{\partial t} = -i\omega c + \frac{K}{2} \int_{-\infty}^{\infty} c(t, \omega') g(\omega') d\omega' \equiv A c. \quad (1.29)$$

Where  $A$  is a linear operator. To discuss the stability of steady solutions we have to find the eigenvalues of  $A$ . The spectrum of  $A$  has continuous and discrete parts.

**Proposition 1.6.** *The discrete spectrum of  $A$  contains non-negative eigenvalues.*

*Proof.* We can find the *discrete* spectrum of  $A$  in this way: let

$$c(t, \omega) = b(\omega) e^{\lambda t}, \quad (1.30)$$

where  $\lambda$  is an eigenvalue. This eigenvalue governs the linear stability of the system. To make the state stable,  $\lambda$  must be negative, since the exponential will decay and when  $t \rightarrow \infty \implies c(t, \omega) \rightarrow 0$ . Hence, the unstable case comes



when  $\lambda$  is positive. Substituting (1.30) into (1.29) and simplifying  $e^{\lambda t}$  on both sides yields

$$\lambda b = -i\omega b + \frac{K}{2} \int_{-\infty}^{\infty} b(\omega')g(\omega')d\omega'. \quad (1.31)$$

The second term on the right-hand side is a constant. Therefore, we can write

$$B = \frac{K}{2} \int_{-\infty}^{\infty} b(\omega')g(\omega')d\omega'. \quad (1.32)$$

If we solve (1.31) for  $b$ , we obtain

$$b(\omega) = \frac{B}{\lambda + i\omega},$$

where we assume  $\lambda + i\omega \neq 0$ . Rewriting equation (1.31) using this expression for  $b$  gives

$$\lambda \frac{B}{\lambda + i\omega} = -i\omega \frac{B}{\lambda + i\omega} + \frac{K}{2} \int_{-\infty}^{\infty} \frac{B}{\lambda + i\omega'}g(\omega')d\omega'. \quad (1.33)$$

This gives  $B = 0$  or  $1 = K/2 \int_{-\infty}^{\infty} \frac{g(\omega')}{\lambda + i\omega'}d\omega'$ . However,  $B$  can not be zero otherwise  $b(\omega) = 0$  and this implies that  $c(t, \omega) = 0$  for all  $\omega$ . This is a contradiction as  $c(t, \omega)$  is an eigenfunction. Therefore, we only consider

$$1 = \frac{K}{2} \int_{-\infty}^{\infty} \frac{g(\omega')}{\lambda + i\omega'}d\omega'. \quad (1.34)$$

At this point, we consider the hypothesis assumed at the beginning:  $g(\omega)$  is even, i.e.,  $g(\omega) = g(-\omega)$ , and is nowhere increasing on  $[0, \infty)$ , in the sense that  $g(\omega) \geq g(v)$  whenever  $\omega \leq v$ . With these assumptions, Eq (1.34) has at most one solution for  $\lambda$  and if it exists, it is real (Theorem 2 [5]). Therefore, Eq. (1.34) can be rewritten as

$$1 = \frac{K}{2} \int_{-\infty}^{\infty} \frac{\lambda}{\lambda^2 + \omega'^2}g(\omega')d\omega'. \quad (1.35)$$

Thus, since the right-hand side of (1.35) can not be negative, all the eigenvalues must satisfy the condition  $\lambda \geq 0$ .  $\square$

Proving this proposition we find out that there can never be any negative eigenvalues and this is a fundamental discovery: the incoherent state of the Kuramoto model can never be linearly stable but it can be either unstable or neutrally stable (unstable if  $\lambda > 0$ , neutrally stable if  $\lambda = 0$ ). So, the next

step is finding the borderline coupling  $K_c$  between these two cases. To do it, consider the limit  $\lambda \rightarrow 0^+$  in (1.35): the term  $\lambda/(\lambda^2 + \omega^2)$  becomes more and more sharply peaked about  $\omega = 0$ , but its integral over  $-\infty < \omega < \infty$  remains equal to  $\pi$ . Therefore, we have

$$\lambda/(\lambda^2 + \omega^2) \longrightarrow \pi\delta(\omega).$$

Thus, the equation (1.35) tends to

$$1 = \frac{1}{2}K_c\pi g(0).$$

In this way we obtain the same value of the critical coupling  $K_c$  of Theorem 1.1.

Following are two explicit examples for the growth rate  $\lambda$ , if  $g(\omega)$  is a sufficiently simple density.

**Example (Uniform density).** *If we consider the uniform density  $g(\omega) = 1/2\gamma$  with  $-\gamma \leq \omega \leq \gamma$  we have*

$$\lambda = \gamma \cot\left(\frac{2\gamma}{K}\right).$$

**Example (Lorentzian density).** *If we consider the Lorentzian density  $g(\omega) = \frac{\gamma}{\pi(\gamma^2 + \omega^2)}$  with  $-\gamma \leq \omega \leq \gamma$  we have*

$$\lambda = \frac{1}{2}K - \gamma.$$

*This value for  $\lambda$  can be found in this way: substitute the Lorentzian distribution into Eq. (1.34),*

$$1 = \frac{K}{2} \int_{-\infty}^{\infty} \frac{\gamma}{\pi(\gamma^2 + \omega^2)(\lambda + i\omega)} d\omega = \frac{K\gamma}{2\pi i} \int_{-\infty}^{\infty} \frac{1}{(\gamma^2 + \omega^2)(\omega - i\lambda)} d\omega.$$

*We solve the right-hand side of this equation with the calculus of residues: the integrand has poles at  $i\gamma$ ,  $-i\gamma$  and  $i\lambda$  with  $\lambda > 0$ . Because  $\lambda$  is positive we close the integration path with half circle on the lower half plane. Calculating the residue of the integrand in  $i\lambda$  and applying the method of residues, we obtain*

$$1 = \frac{K}{2(\lambda + \gamma)}.$$

Now let's discuss the *continuous* spectrum.

**Proposition 1.7.** *The continuous spectrum of  $A$  is pure imaginary,  $\{i\omega : \omega \in \text{support}(g)\}$ , and it corresponds to a continuous family of neutral modes.*

*Proof.* For definition, the continuous part of the spectrum of  $A$  is defined as the set of complex numbers such that the operator  $A - \lambda I$  is not surjective. So, we need to consider

$$-(\lambda + i\omega)b(\omega) + \frac{K}{2} \int_{-\infty}^{\infty} b(\omega')g(\omega')d\omega' = f(\omega), \quad (1.36)$$

for fixed  $\lambda$  and for an arbitrary function  $f(\omega)$ . If Eq.(1.36) is solvable for all  $b(\omega)$   $\lambda$  is not in the continuous spectrum. As we already noted, the integral does not depend on  $\omega$ , it is a constant. Therefore we denote this integral by  $B$ , as we did in the proof of Proposition 1.6. Thus, if  $\lambda + i\omega = 0$ , Eq. (1.36) is not solvable for all  $f(\omega)$ : it is solvable only for constant functions. Consequently we can conclude that the continuous spectrum contains  $\{i\omega : \omega \in \text{support}(g)\}$ .

Now we demonstrate that nothing else is contained in the continuous spectrum. Let's suppose that there is an eigenvalue  $\lambda$  in the continuous spectrum but not in  $\{i\omega : \omega \in \text{support}(g)\}$ . Since  $\lambda + i\omega \neq 0$ , we can solve Eq. (1.36) for  $b(\omega)$ . We obtain

$$b(\omega) = \frac{B - f(\omega)}{\lambda + i\omega}, \quad (1.37)$$

where  $B = \frac{K}{2} \int_{-\infty}^{\infty} b(\omega')g(\omega')d\omega'$ . Substituting (1.37) into the expression for  $B$  we have

$$\begin{aligned} B &= \frac{K}{2} \int_{-\infty}^{\infty} \left[ \frac{B - f(\omega')}{\lambda + i\omega'} \right] g(\omega')d\omega' \\ &= \frac{BK}{2} \int_{-\infty}^{\infty} \left[ \frac{g(\omega')}{\lambda + i\omega'} \right] d\omega' - \frac{K}{2} \int_{-\infty}^{\infty} \left[ \frac{f(\omega')}{\lambda + i\omega'} \right] g(\omega')d\omega'. \end{aligned} \quad (1.38)$$

In this way, we obtain

$$B \left( 1 - \frac{K}{2} \int_{-\infty}^{\infty} \frac{g(\omega')}{\lambda + i\omega'} d\omega' \right) = -\frac{K}{2} \int_{-\infty}^{\infty} \left[ \frac{f(\omega')}{\lambda + i\omega'} \right] g(\omega')d\omega'. \quad (1.39)$$

We assume that  $\lambda$  is not in the discrete spectrum. Thus, from equation (1.34) it follows that the coefficient of  $B$  is not zero. Therefore, Eq. (1.39) is solvable for  $B$ . This implies that  $\lambda$  is not in the continuous spectrum. Thus, we have showed that the continuous spectrum is  $\{i\omega : \omega \in \text{support}(g)\}$ .  $\square$

**Observation 1.10.** *The proposition that we have just proved implies neutral stability.*

**Observation 1.11.** We can imagine an initial perturbation  $\eta(\theta, \omega, t = 0)$  supported on a sliver of exactly one frequency  $\omega = \omega_0$ , so we disturb the part of the oscillators which have intrinsic frequency  $\omega_0$  and leave the rest alone in their incoherent state. The corresponding amplitude  $c(0, \omega)$  is zero for all the oscillators which have frequencies  $\omega \neq \omega_0$  because they are not disturb. Instead, in the case of  $\omega = \omega_0$ , we can set  $c(0, \omega_0) = 1$  because the equation (1.29) is linear. For this sliver perturbation, the integral in (1.29) vanishes so the equation become

$$Ac = i\omega_0 c.$$

In this form we can note that  $c(0, \omega)$  is an eigenfunction with pure imaginary eigenvalue  $i\omega_0$ .

Therefore, the linearization about the incoherent state of the Kuramoto model has a purely imaginary continuous spectrum for  $K < K_c = \frac{2}{\pi g(0)}$  where the discrete spectrum is empty. When  $K$  increases, a real positive eigenvalue  $\lambda$  appears from the continuous spectrum and moves into the right half plane for  $K > K_c$ , as we can see in the figure below.

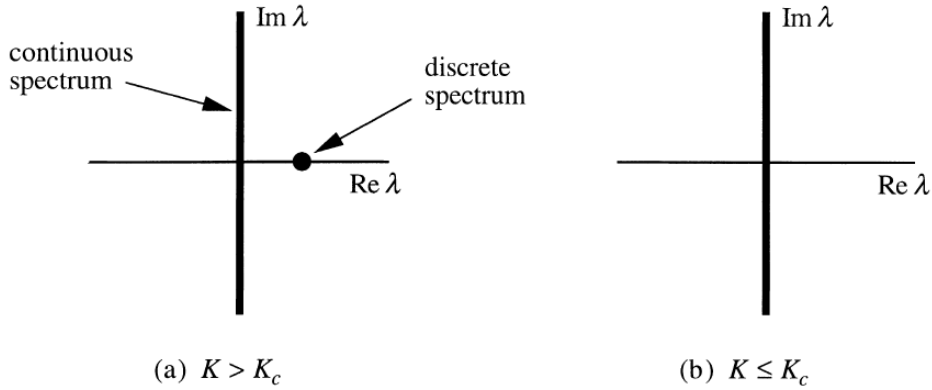


Figure 1.4: Spectrum of  $A$  that governs the linear stability of the incoherent state  $\rho_0 \equiv 1/2\pi$ . (a) For  $K > K_c$  the incoherent state is unstable, thanks to the discrete eigenvalue  $\lambda > 0$ . This eigenvalue pops out of the continuous spectrum at  $K = K_c$ . (b) For  $K \leq K_c$ , the discrete spectrum is empty and the incoherent state is neutrally stable.

We have just proved the following Theorem:

**Theorem 1.4.** *The incoherent state is neutrally stable for  $K < K_c$  and unstable for  $K > K_c$ .*

What happens when  $K$  decreases through  $K_c$ ? We can think that the eigenvalue  $\lambda$  should move toward the continuous spectrum, collide with it, then pop out the back. But it do not, it just disappears! Another weird thing is that the explicit formulas for  $\lambda$  simply predict, incorrectly, that  $\lambda$  goes negative for  $K < K_c$ . Thanks to some simulations for  $K < K_c$  it seems to show that  $r(t)$  decays exponentially and the decay rate is exactly the negative  $\lambda$  found using explicit formulas. We need to find an equation governing the evolution of  $r(t)$ . Putting together Eq. (1.27), the expression of  $\eta$  as a Fourier series and Eq. (1.21) we have

$$r(t) = 2\pi\epsilon \left| \int_{-\infty}^{\infty} c(t, \omega) g(\omega) d\omega \right|. \quad (1.40)$$

Now, we introduce the notation

$$R(t) = \int_{-\infty}^{\infty} c(t, \omega) g(\omega) d\omega \quad (1.41)$$

and we solve the first-order linear ordinary differential equation (1.29) in terms of  $R(t)$  and the initial condition  $c_0(\omega) \equiv c(0, \omega)$ . Inserting the result for  $c(t, \omega)$  into (1.41) gives the linear integral equation

$$R(t) = (\widehat{c_0 g})(t) + \frac{K}{2} \int_0^t R(t - \tau) \widehat{g}(\tau) d\tau, \quad (1.42)$$

where the hat denotes Fourier transform.

**Definition 1.23.** A function  $g$  belongs to  $L^1(\mathbb{R}, \mathbb{C})$  if

$$\int_{-\infty}^{\infty} |g(\omega)| d\omega < \infty.$$

**Definition 1.24.** Suppose  $g \in L^1(\mathbb{R}, \mathbb{C})$ , its Fourier transform is the function  $\widehat{g} : \mathbb{R} \rightarrow \mathbb{C}$  defined by

$$\widehat{g}(t) = \int_{-\infty}^{\infty} g(\omega) e^{-i\omega t} d\omega.$$

At this point, the next goal is solving (1.42). We can use Laplace transform and then apply the inverse Laplace transform.

**Definition 1.25.** Let  $f(t)$  be a function of  $t$  specified for  $t > 0$ . Then the Laplace transform of  $f(t)$  is defined by

$$f(s) = \int_0^{\infty} e^{-st} f(t) dt,$$

where  $s$  is complex.

We obtain

$$R(t) = \frac{1}{2\pi i} \int_{\Gamma} \frac{(c_0 g)^*(s)}{1 - \frac{1}{2} K g^*(s)} e^{st} ds, \quad (1.43)$$

where the contour  $\Gamma$  is a vertical line to the right of any singularities of the integrand, and the asterisk denotes an operation related to the Hilbert transform:

$$f^*(s) \equiv \int_{-\infty}^{\infty} \frac{f(\omega) d\omega}{s + i\omega}.$$

We have  $g^*(s) \equiv \int_{-\infty}^{\infty} \frac{g(\omega) d\omega}{s + i\omega}$  and from Eq. (1.34) we can see that this integral is equal to  $\frac{2}{K}$  if  $s$  is in the discrete spectrum of  $A$  and substituting  $g^*(s) = \frac{2}{K}$  into (1.43) we see that the denominator in (1.43) vanishes. In the case  $K < K_c$ , the discrete spectrum is empty, as we stated previously, so the denominator never vanishes.

**Example.** *If we consider the extremely special initial condition  $c_0(\omega) \equiv 1$  and the Lorentzian distribution  $g(\omega) = \frac{\gamma}{\pi(\gamma^2 + \omega^2)}$ , we have  $\hat{g}(t) = e^{-|\gamma t|}$  and the explicit solution of (1.43) is*

$$R(t) = e^{(\frac{1}{2}K - \gamma)t}, \quad t \geq 0.$$

*From this solution we discover that  $R(t)$ , and hence  $r(t)$ , decays exponentially if  $K < K_c = 2\gamma$ , even though the incoherent state is neutrally stable.*

**Example.** *In the case of the uniform density  $g(\omega) = 1/2\gamma$ , with  $-\gamma \leq \omega \leq \gamma$ , we find*

$$R(t) \sim \left( \frac{-16\gamma}{K^2} \right) \frac{\sin \gamma t}{t \ln^2 t} \quad \text{as } t \rightarrow \infty$$

*for  $K < K_c$ , which is a much slower decay than the other one.*

**Observation 1.12.** *In the case  $K < K_c$  the asymptotic behavior of  $R(t)$  depends on the support of  $g(\omega)$ . If  $g(\omega)$  has a compact support, as the finite interval  $[-\gamma, \gamma]$ , we have that  $R(t) \rightarrow 0$  as  $t \rightarrow \infty$ , but the decay is always slower than exponential. On the other hand, if  $g(\omega)$  is supported on the whole real line, the asymptotic behavior of  $R(t)$  can be more particular:  $R(t)$  can take any form with a correct choice of  $c_0$  but in the best-behaved case where  $g(\omega)$  and  $c_0(\omega)$  are entire functions,  $R(t)$  is a sum of decaying exponentials.*

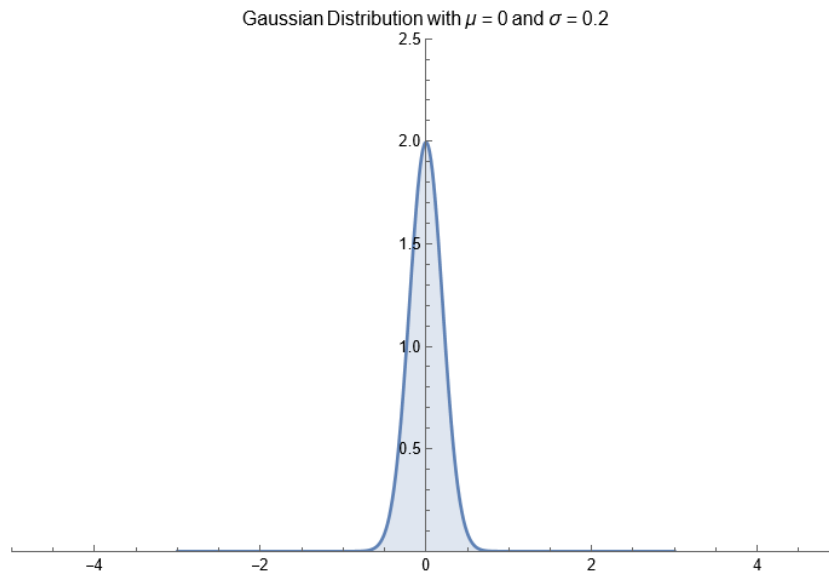
## 1.5 Simulations

In this last section I show some theoretical results, proved in the previous sections, through numerical simulations. I used Wolfram Mathematica to do that.

To do the simulations I assumed that the natural frequencies are distributed according to the Gaussian distribution with mean  $\mu = 0$  and deviation  $\sigma = 0.2$ . The density of the Gaussian distribution is

$$g(x) = \frac{1}{\sqrt{2\pi\sigma^2}} e^{-\frac{(x-\mu)^2}{2\sigma^2}},$$

with  $x \in \mathbb{R}$ . I opted for this distribution because it satisfies all the properties that the density of the frequencies must have in the Kuramoto model: the Gaussian density is unimodal, symmetric about its mean and nowhere increasing on  $[0, \infty]$  as we can see in the graph below.



I assumed also that the initial phases of oscillators are distributed according to the same density. I considered  $N = 250$  oscillators. In order to solve the differential equations (1.3) of the Kuramoto model I used the command `NDSolve` from Mathematica and I considered different values of  $K$  ( $K \in \{0, 0.1, 0.2, 0.3, 0.4, 0.5, 0.6, 0.7, 0.8\}$ ) to visualize how the behavior of the oscillators changes with the increase of  $K$ .

We can note, in the figure 1.5 below, that for small values of the coupling constant  $K$ , the oscillators, represented by black points on the unit circle, are scattered around the circle. This means that they run incoherently, they are not synchronized. In fact, the orange arrow, which represents the radius  $r$ , is *little*. We have  $r \approx 0$ , as we expected from the theory. As the value of coupling strength increases the oscillators are getting closer and  $r \approx 1$ . The population acts like a giant single oscillator.

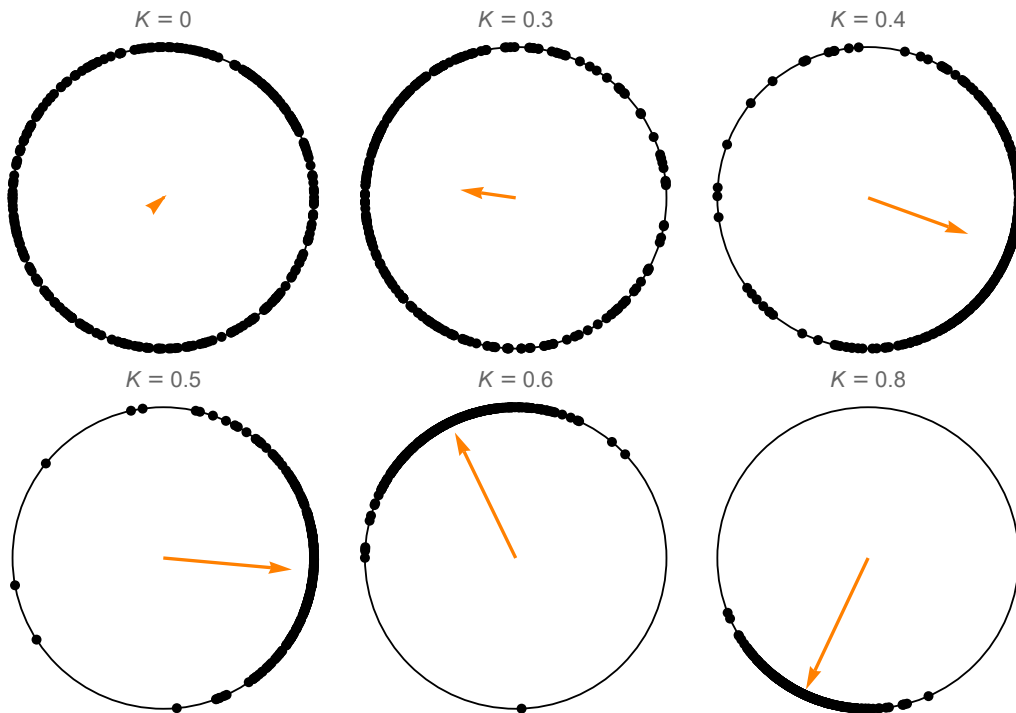


Figure 1.5: Oscillators' plot on the unit circle for different values of  $K$ . For  $K = 0$  we have  $r \approx 0$  that means that the oscillators are not synchronized, for  $K = 0.4$  we have  $0 < r < 1$  so the oscillators are partially synchronized, for  $K = 0.8$  we have  $r \approx 1$  that means that the oscillators are almost fully synchronized.

Then, I showed the phase transition of the Kuramoto model. For the Theorem 1.1 the threshold value in the case of Gaussian distribution with mean  $\mu = 0$  and deviation  $\sigma = 0.2$  is

$$K_c = \frac{2}{\pi g(0)} = 0.319154.$$

We can note, in the figure below, that for the first values of  $K$  we have  $r \approx 0$ , then, near the critical point  $K_c$ ,  $r$  begin to increase and getting closer and



closer to 1. Therefore, at  $K \approx K_c$  the phase transition occurs and the oscillators begin to synchronize. With greater values of number of oscillators and  $t_{\text{final}}$  the graphs are even better.

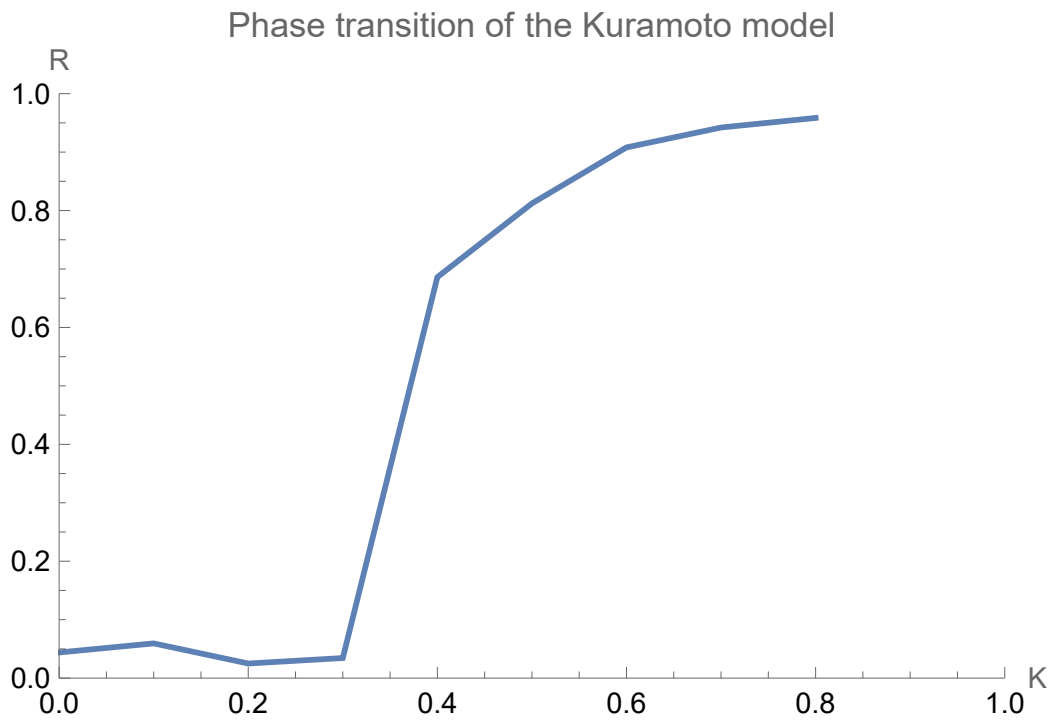


Figure 1.6: At  $K \approx 0.3$  the phase transition occurs, for  $K < K_c$  the oscillators run incoherently, for  $K > K_c$  they start to synchronize.



# Chapter 2

## Kuramoto model with adding noise

In this chapter of the thesis, to get a more complete analysis of the Kuramoto model, we consider the relevance of noise: noise, due a variety of reasons, might affect the system of oscillators in equation (1.3). For instance the behavior of an array of Josephson junctions could be greatly affected by thermal noise so it is important to study how random noise can change the synchronization behavior seen in the Kuramoto model. The model with the presence of noise takes the name of Sakaguchi-Kuramoto model because was Sakaguchi to extend the KM allowing rapid stochastic fluctuations in the natural frequencies.

### 2.1 The Sakaguchi-Kuramoto model

The system of equations that describes the Sakaguchi-Kuramoto model is

$$d\theta_i = \left( \omega_i + \frac{K}{N} \sum_{j=1}^N \sin(\theta_j - \theta_i) \right) dt + \sigma dW_i, \quad i = 1, \dots, N, \quad (2.1)$$

where  $W$  denotes a Wiener process, also called Brownian motion.

The system (2.1) is a system of stochastic differential equations. For a rigorous introduction see [6]. For our purpose it suffices to say that the system (2.1), for  $dt$  small, can be approximated by the following system of differential equations:

**Definition 2.1** (Sakaguchi model). *The system of equations of the Sakaguchi-*

Kuramoto model that we are going to consider is

$$d\theta_i = \left( \omega_i + \frac{K}{N} \sum_{j=1}^N \sin(\theta_j - \theta_i) \right) dt + \sqrt{\sigma^2 dt} X_i, \quad i = 1, \dots, N, \quad (2.2)$$

where  $X_1, \dots, X_N$  are independent random variables distributed according to the Standard Gaussian distribution, i.e.  $X_i \sim N(0, 1)$   $i = 1, \dots, N$ .

The oscillators' distribution function  $\rho(\theta, t, \omega)$  satisfy the nonlinear Fokker-Planck equation

$$\frac{\partial \rho}{\partial t} = \frac{\sigma^2}{2} \frac{\partial^2 \rho}{\partial \theta^2} - \frac{\partial}{\partial \theta}(\rho v), \quad (2.3)$$

where the parameter  $\frac{\sigma^2}{2}$  sizes the strength of noise and  $v(\theta, t, \omega)$ ,  $r(t)$  and  $\psi(t)$  are given by (1.20) and (1.21).

**Observation 2.1.** *The Sakaguchi's Fokker-Planck equation tell us how the oscillator density function  $\rho(\theta, t, \omega)$  evolves in time and we can note that it reduces to the continuum limit of the Kuramoto model when  $\sigma = 0$ , so when there is no noise.*

### 2.1.1 Derivation of Fokker-Planck equation

**Theorem 2.1.** *The Fokker-Planck equation for the Sakaguchi model is*

$$\frac{\partial \rho}{\partial t} = \frac{\sigma^2}{2} \frac{\partial^2 \rho}{\partial \theta^2} - \frac{\partial}{\partial \theta}(\rho v), \quad (2.4)$$

where  $v(\theta, t, \omega)$ ,  $r(t)$  and  $\psi(t)$  are given by (1.20) and (1.21).

*Proof.* From (1.3) we know that

$$v_i = \omega_i + \frac{K}{N} \sum_{j=1}^N \sin(\theta_j - \theta_i), \quad (2.5)$$

which is the instantaneous angular velocity of oscillator  $i$  in the absence of noise. Substituting (2.5) into (2.2) we obtain

$$d\theta_i = v_i dt + \sqrt{\sigma^2 dt} X_i, \quad i = 1, \dots, N. \quad (2.6)$$

We know that

$$\int f(\theta) \rho(\theta, \omega, t) d\theta = \langle f(\theta) \rangle \quad (2.7)$$

and differentiating it, we obtain

$$\int f(\theta) \frac{\partial \rho}{\partial t} d\theta = \left\langle \frac{df(\theta)}{dt} \right\rangle. \quad (2.8)$$

Now, we expand  $df$  to the second order

$$df = \frac{\partial f}{\partial \theta} d\theta + \frac{\partial^2 f}{\partial \theta^2} \frac{(d\theta)^2}{2}. \quad (2.9)$$

Substituting (2.6) into (2.9) gives

$$\begin{aligned} df &= \frac{\partial f}{\partial \theta} (vdt + \sqrt{\sigma^2 dt} X) \\ &+ \frac{\partial^2 f}{\partial \theta^2} \frac{(v^2 dt^2 + \sigma^2 dt X^2 + 2vdt\sqrt{\sigma^2 dt} X)}{2}. \end{aligned} \quad (2.10)$$

We drop terms with factors of  $(dt)^2$  or smaller obtaining

$$df = \frac{\partial f}{\partial \theta} (vdt + \sqrt{\sigma^2 dt} X) + \frac{\partial^2 f}{\partial \theta^2} \frac{\sigma^2 dt}{2} X^2. \quad (2.11)$$

At this point, we can note that

$$\left\langle \sqrt{\sigma^2 dt} X \right\rangle = \left\langle \sqrt{\sigma^2 dt} \right\rangle \langle X \rangle = 0, \quad (2.12)$$

because the mean of the random variable  $X$  is 0 by definition. We can also note that

$$\langle X^2 \rangle = 1 \quad (2.13)$$

since the average of the square is equal to the variance when the mean is zero. Now, we substitute (2.11) into (2.8) and we find

$$\int f(\theta) \frac{\partial \rho}{\partial t} d\theta = \left\langle \frac{df}{d\theta} v + \frac{\sigma^2}{2} \frac{d^2 f}{d\theta^2} \right\rangle. \quad (2.14)$$

Now we express the right-hand side of this equation as an integration over phase space:

$$\int f(\theta) \frac{\partial \rho}{\partial t} d\theta = \int \left( \frac{df}{d\theta} v + \frac{\sigma^2}{2} \frac{d^2 f}{d\theta^2} \right) \rho d\theta. \quad (2.15)$$

We integrate the right-hand side by parts and we drop the surface terms (since we have periodic boundaries). In this way we obtain

$$\int f(\theta) \frac{\partial \rho}{\partial t} d\theta = \int f(\theta) \left( -\frac{\partial \rho}{\partial \theta} v + \frac{\sigma^2}{2} \frac{\partial^2 \rho}{\partial \theta^2} \right) d\theta. \quad (2.16)$$

So, it must be that

$$\frac{\partial \rho}{\partial t} = \frac{\sigma^2}{2} \frac{\partial^2 \rho}{\partial \theta^2} - \frac{\partial}{\partial \theta} (\rho v). \quad (2.17)$$

Thus, we obtain the Fokker-Planck equation for the Kuramoto model.  $\square$

## 2.2 Stability of the incoherent state

In order to investigate the synchronization behavior of the Kuramoto model with noise, we study the incoherent state  $\rho_0(\theta, \omega) \equiv \frac{1}{2\pi}$  as we did in the first chapter. We want to discover the stability properties of the incoherent state. Since the incoherent state, as we have seen, corresponds to a completely unsynchronized state, if we find the situations in which this incoherent state just becomes unstable, we have found the situations where phase synchronization just starts to take place.

With this aim, we substitute the perturbed distribution (1.27) and the expression of  $\eta$  as a Fourier series into the Fokker-Planck equation (2.3) and we find

$$\frac{\partial c}{\partial t} = -\left(\frac{\sigma^2}{2} + i\omega\right)c + \frac{K}{2} \int_{-\infty}^{\infty} c(t, \omega')g(\omega')d\omega'. \quad (2.18)$$

The linear operator  $L$  describing the right hand side of (2.18) is given by

$$Lc = -\left(\frac{\sigma^2}{2} + i\omega\right)c + \frac{K}{2} \int_{-\infty}^{\infty} c(t, \omega')g(\omega')d\omega'. \quad (2.19)$$

This equation has both a discrete and continuous spectrum. To find them we proceed in the same way we did in the case of no noise [4].

**Proposition 2.1.** *The discrete spectrum in case of presence of noise is not the same when there is no noise.*

*Proof.* We look for separable solutions of (2.18) of the form

$$c(t, \omega) = b(\omega)e^{\lambda t}, \quad (2.20)$$

where the eigenvalue  $\lambda$  will tell us the stability of  $c$  and therefore the stability of  $r$ . If  $\lambda > 0$  then  $c$  grows exponentially in time and consequently  $r$  grows exponentially because in the Proposition 1.5 we have demonstrated that  $r$  depends only on  $c$ . So  $\lambda > 0$  means that the incoherent state is unstable. If  $\lambda < 0$ ,  $c$  decays, and  $r$  shrinks back down to zero, meaning the incoherent state is stable. To solve for  $\lambda$  we use the eigenvalue equation

$$(L - \lambda I)c = (L - \lambda I)be^{\lambda t} = 0, \quad (2.21)$$

where  $b$  is not allowed to be zero because otherwise  $c$  is zero and it is not possible since  $L$  is an eigenfunction. Substitute (2.20) into (2.18) and dividing through by  $e^{\lambda t}$  we obtain

$$\lambda b = -\left(\frac{\sigma^2}{2} + i\omega\right)b + \frac{K}{2} \int_{-\infty}^{\infty} b(\omega')g(\omega')d\omega'. \quad (2.22)$$

Since the integral in Eq. (2.22) is just some constant, we can call it

$$A = \frac{K}{2} \int_{-\infty}^{\infty} b(\omega') g(\omega') d\omega', \quad (2.23)$$

and then solve for  $b$  in Eq. (2.22) we find

$$b(\omega) = \frac{A}{\lambda + \frac{\sigma^2}{2} + i\omega}. \quad (2.24)$$

Then we substitute (2.24) into (2.23), obtaining

$$A = \frac{K}{2} \int_{-\infty}^{\infty} \frac{Ag(\omega')}{\lambda + \frac{\sigma^2}{2} + i\omega'} d\omega' \quad (2.25)$$

We do not consider the solution  $A = 0$  because it implies  $b = 0$  and therefore  $c = 0$  which is not possible. Thus, we have

$$1 = \frac{K}{2} \int_{-\infty}^{\infty} \frac{g(\omega')}{\lambda + \frac{\sigma^2}{2} + i\omega'} d\omega'. \quad (2.26)$$

If we assume that  $g(\omega)$  is even and it never increases on  $[0, \infty)$ , which is true for the distributions that we are looking at, then, as we have already said, there is at most one solution for  $\lambda$ , and if a solution exists, it is real. This means we can multiply and divide the integrand in the Eq. (2.26) by the complex conjugate of the denominator to get

$$1 = \frac{K}{2} \int_{-\infty}^{\infty} \frac{\lambda + \frac{\sigma^2}{2} - i\omega'}{(\lambda + \frac{\sigma^2}{2})^2 + \omega'^2} g(\omega') d\omega' \quad (2.27)$$

and the imaginary part will integrate to zero because it is an odd function of  $\omega'$ . Therefore, we obtain

$$1 = \frac{K}{2} \int_{-\infty}^{\infty} \frac{\lambda + \frac{\sigma^2}{2}}{(\lambda + \frac{\sigma^2}{2})^2 + \omega'^2} g(\omega') d\omega'. \quad (2.28)$$

Reached this point, we can note that any eigenvalue  $\lambda$  must satisfy the inequality

$$\lambda > -\frac{\sigma^2}{2}$$

so that the right side of Eq. (2.28) can be positive. Since  $\frac{\sigma^2}{2} > 0$ ,  $\lambda$  can be negative, therefore, we can conclude that the incoherent state can be stable (instead in the case of no noise the incoherent state cannot be linearly stable, only neutrally stable).  $\square$

**Observation 2.2.** Equation (2.28) is the one of the main results of this chapter. It shows how the eigenvalue  $\lambda$  depends on the noise strength, the coupling strength  $K$  and the frequency density  $g(\omega)$ .

At this point, we can show the following result:

**Theorem 2.2.** The critical coupling point at which stability of incoherent state is lost and phase transition occurs is

$$\hat{K}_c = 2 \left[ \int_{-\infty}^{\infty} \frac{\frac{\sigma^2}{2}}{\frac{\sigma^4}{4} + \omega'^2} g(\omega') d\omega' \right]^{-1}. \quad (2.29)$$

*Proof.* Setting  $\lambda = 0$  in Eq. (2.28). □

For some special cases of the distribution of natural frequencies  $g(\omega)$  the eigenvalue  $\lambda$  can be found explicitly. Here are some examples.

**Example (Identical oscillators).** If we consider identical oscillators,  $g(\omega) = \delta(\omega)$ , that it means that all the oscillators have the same natural frequency, the equation (2.28) becomes

$$\begin{aligned} 1 &= \frac{K}{2} \int_{-\infty}^{\infty} \frac{\lambda + \frac{\sigma^2}{2}}{(\lambda + \frac{\sigma^2}{2})^2 + \omega'^2} \delta(\omega') d\omega' \\ &= \frac{K}{2} \frac{\lambda + \frac{\sigma^2}{2}}{(\lambda + \frac{\sigma^2}{2})^2} \\ &= \frac{K}{2(\lambda + \frac{\sigma^2}{2})}. \end{aligned}$$

Therefore,

$$\lambda = \frac{K - \sigma^2}{2}.$$

And if we set  $\lambda = 0$  we find

$$\hat{K}_c = \sigma^2.$$

**Example (Uniform density).** If we consider the uniform density

$$g(\omega) = \begin{cases} \frac{1}{2\gamma} & -\gamma \leq \omega \leq \gamma \\ 0 & \text{elsewhere} \end{cases}$$

we find

$$\lambda = \gamma \cot \frac{2\gamma}{K} - \frac{\sigma^2}{2}.$$



By setting  $\lambda = 0$  we obtain the critical coupling

$$\hat{K}_c = \frac{2\gamma}{\arctan \frac{\gamma}{\sigma^2/2}}.$$

**Example** (Lorentzian density). *If we consider the Lorentzian density we find*

$$\lambda = \frac{K - \sigma^2}{2} - \gamma.$$

By setting  $\lambda = 0$  we obtain the critical coupling

$$\hat{K}_c = \sigma^2 + 2\gamma.$$

Now we finish the analysis of stability of incoherent state studying the continuous spectrum.

**Proposition 2.2.** *The continuous spectrum of  $L$  is*

$$\left\{ -\frac{\sigma^2}{2} - i\omega : \omega \in \text{support}(g) \right\}.$$

*Proof.* For definition, the continuous spectrum of  $L$  is the set of complex number  $\lambda$  such that the operator  $L - \lambda I$  is not surjective. Therefore, we are led to consider this equation

$$-\left(\lambda + \frac{\sigma^2}{2} + i\omega\right)b + \frac{K}{2} \int_{-\infty}^{\infty} b(\omega)g(\omega)d\omega = f(\omega), \quad (2.30)$$

for fixed  $\lambda$  and for an arbitrary function  $f(\omega)$ . In the case that Eq. (2.30) can be solved for all  $b(\omega)$   $\lambda$  is not in the continuous spectrum. As we already noted, the integral in (2.30) does not depend on  $\omega$ . So we denote this integral again by  $A$ . If  $\lambda + \frac{\sigma^2}{2} + i\omega = 0$  for some  $\omega$  in the support of  $g$  then equation (2.30) is not solvable in general: it would be solvable only for constant functions. Thus we can conclude that the continuous spectrum contains

$$\left\{ -\frac{\sigma^2}{2} - i\omega : \omega \in \text{support}(g) \right\}.$$

Now we prove that this is the entire continuous spectrum. We suppose that there is an eigenvalue  $\lambda$  that is not in the discrete spectrum and  $\lambda \neq -\frac{\sigma^2}{2} - i\omega$ . Since  $\lambda + \frac{\sigma^2}{2} + i\omega \neq 0$ , we can solve Eq. (2.30) for  $b(\omega)$ . We obtain

$$b(\omega) = \frac{A - f(\omega)}{\lambda + \frac{\sigma^2}{2} + i\omega}. \quad (2.31)$$

Substituting (2.31) into the integral  $A$  we have

$$\begin{aligned} A &= \frac{K}{2} \int_{-\infty}^{\infty} \left[ \frac{A - f(\omega')}{\lambda + \frac{\sigma^2}{2} + i\omega'} \right] g(\omega') d\omega' \\ &= \frac{AK}{2} \int_{-\infty}^{\infty} \left[ \frac{g(\omega')}{\lambda + \frac{\sigma^2}{2} + i\omega'} \right] d\omega' - \frac{K}{2} \int_{-\infty}^{\infty} \left[ \frac{f(\omega')}{\lambda + \frac{\sigma^2}{2} + i\omega'} \right] g(\omega') d\omega'. \end{aligned} \quad (2.32)$$

In this way, we obtain

$$A \left( 1 - \frac{K}{2} \int_{-\infty}^{\infty} \frac{g(\omega')}{\lambda + \frac{\sigma^2}{2} + i\omega'} d\omega' \right) = -\frac{K}{2} \int_{-\infty}^{\infty} \left[ \frac{f(\omega')}{\lambda + \frac{\sigma^2}{2} + i\omega'} \right] g(\omega') d\omega'. \quad (2.33)$$

We have assumed that  $\lambda$  is not in the discrete spectrum. Thus, from equation (2.26) it follows that the coefficient of  $A$  is not zero. Therefore, Eq. (2.33) is solvable for  $A$ . This implies that  $\lambda$  is not in the continuous spectrum. Thus, we have showed that the continuous spectrum is

$$\left\{ -\frac{\sigma^2}{2} - i\omega : \omega \in \text{support}(g) \right\}.$$

□

**Observation 2.3.** *When  $\frac{\sigma^2}{2} > 0$  the continuous spectrum lies in the left-half plane. Instead, in the case  $\frac{\sigma^2}{2} = 0$  the continuous spectrum lies on the imaginary axis.*

In the figure 2.1 is represented the discrete and the continuous spectrum for a frequency density  $g(\omega)$  with support  $[-\gamma, \gamma]$ . The figure shows that for  $\frac{\sigma^2}{2} > 0$ , the continuous spectrum is a vertical line segment in the left half-plane, irrespective of the value of  $K$ . Thus, the modes corresponding to the continuous spectrum never cause instability. In contrast, the discrete spectrum depends strongly on  $K$ . When  $K > \hat{K}_c$  (Fig. 1a) the fundamental mode is unstable because  $\lambda > 0$ . As  $K$  decreases, the eigenvalue moves to the left and consequently the fundamental mode becomes neutrally stable because  $\lambda = 0$  (Fig. 1b) and then linearly stable because  $\lambda < 0$  (Fig. 1c). Finally, in Fig. 1d, the discrete spectrum is absorbed by the continuous spectrum and disappears.

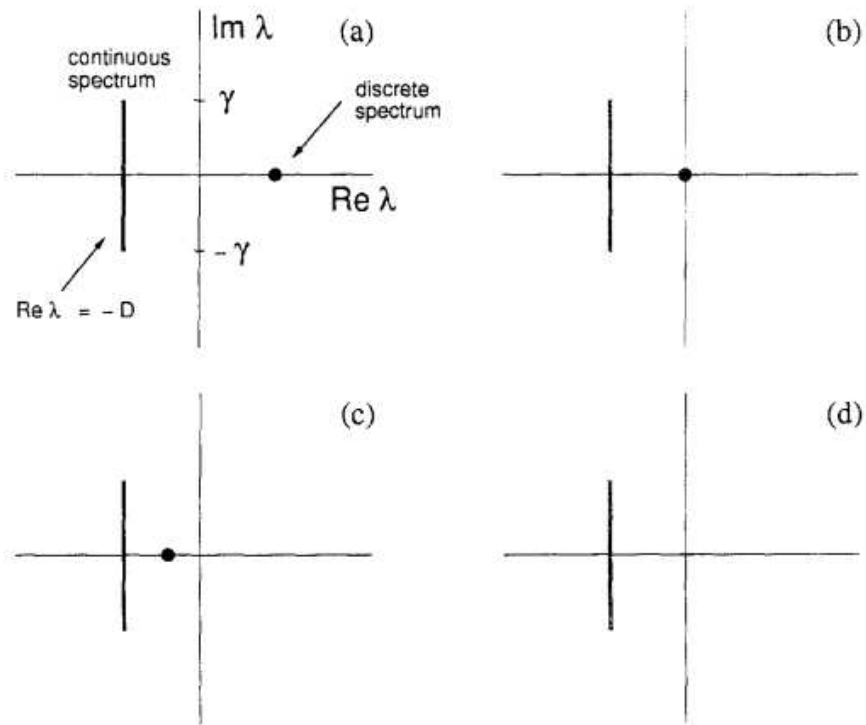


Figure 2.1: Representation of discrete and continuous spectrum when there is noise for different values of  $K$ . In the figure  $D = \frac{\sigma^2}{2}$ .

## 2.3 Simulations

In this last section of the chapter, as I did in the first chapter, I show some theoretical results, proved in the previous pages of the chapter, through numerical simulations on Mathematica. In this simulation I consider the presence of noise.

The assumptions are the same of the other simulation, so the natural frequencies of the oscillators are distributed according to the Gaussian distribution with mean  $\mu = 0$  and deviation  $\sigma = 0.2$ . The initial phases of oscillators are distributed according to the same distribution and I considered  $N = 250$  oscillators. I take into account the same hypothesis to compare the results with and without noise. In the simulation with noise I consider larger values of  $K$  because, we can note, from the figures in this section, that in the case of noise to reach a similar value of  $r$  of the case with no noise, we need a larger value of coupling strength. In fact, in the figure 2.3, we can observe that for  $K = 0.8$  the oscillators are not as synchronized as they were in case there was no noise.

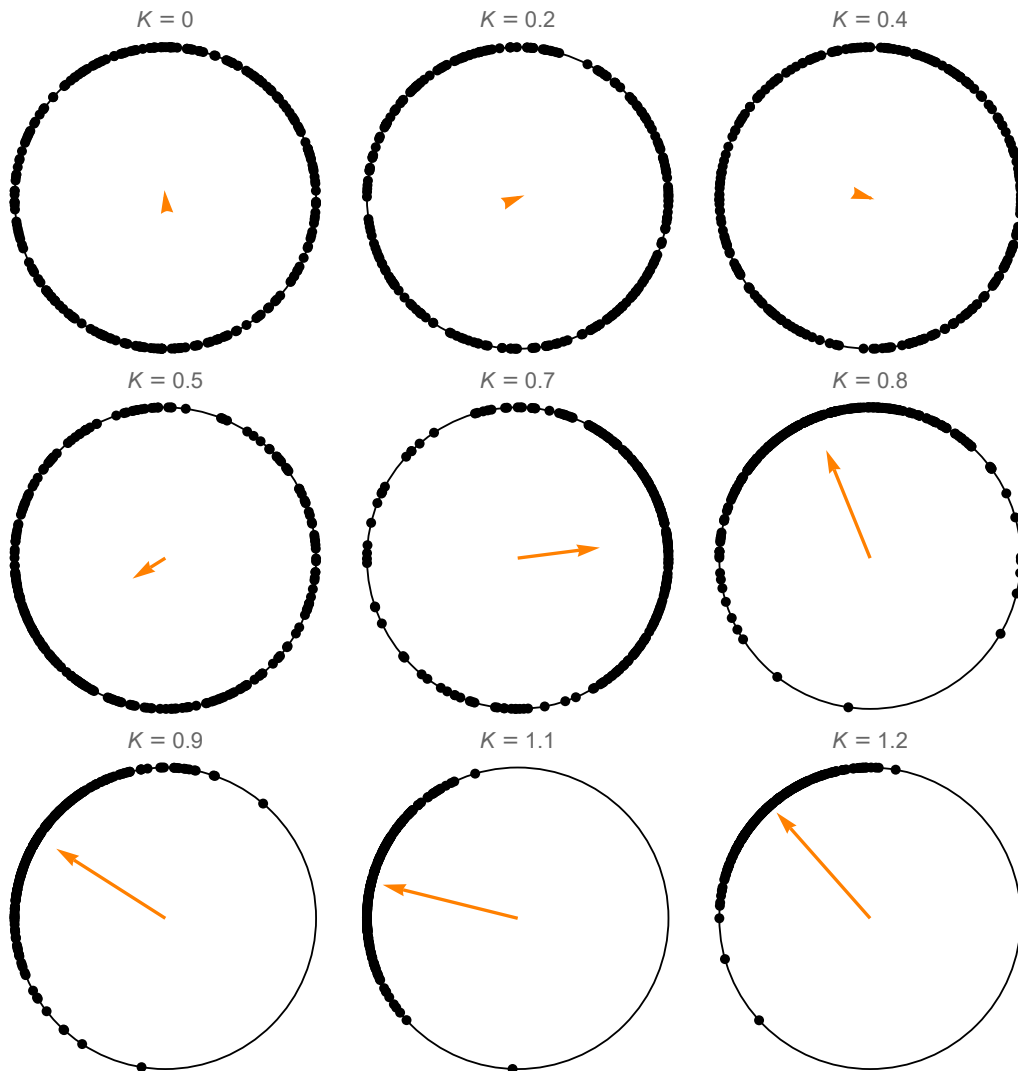


Figure 2.2: Oscillators' plot on the unit circle for different values of  $K$  with presence of noise. For  $K \in \{0, 0.2, 0.4\}$  we have  $r \approx 0$  that means that the oscillators are completely unsynchronized. For  $K = 0.7$  we have  $0 < r < 1$  that means that the oscillators are partially synchronized in fact the *points* on the unit circle are getting closer. For  $K = 1.2$  we have  $r \approx 1$  that means that the oscillators are almost fully synchronized, the oscillators act like a single huge oscillator.

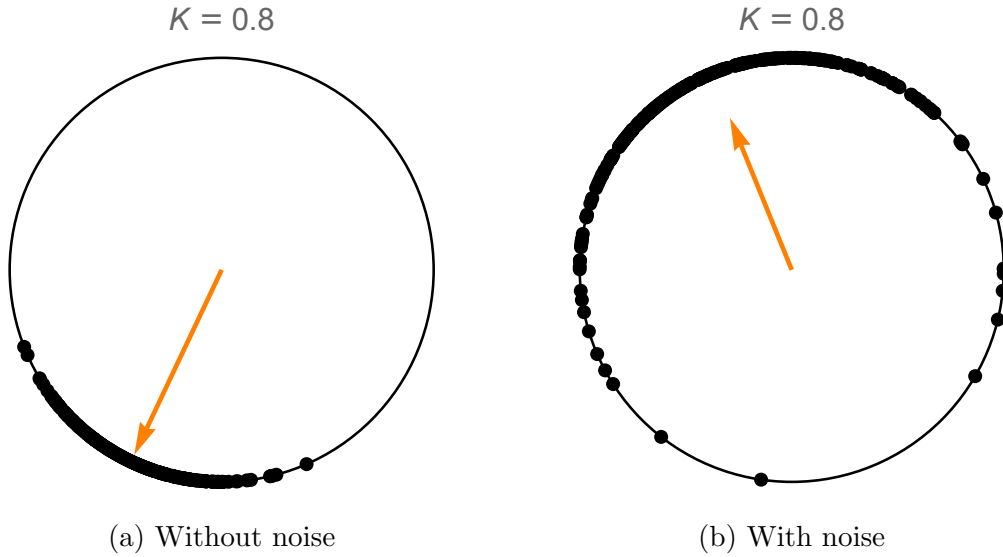


Figure 2.3: Representation of oscillators on the unit circle for  $K = 0.8$  without noise, fig.a, and with noise, fig.b. For the same value of coupling constant the synchronization behavior of oscillators is different: the oscillators are *more* synchronized when there is no noise.

Finally, I showed the phase transition of the Sakaguchi-Kuramoto model. I considered as value of the noise strength

$$\frac{\sigma^2}{2} = 0.05,$$

where the  $\sigma$  that appears in the formula is not the deviation of the Gaussian distribution but is the constant that appears in Eq. (2.2). For the Theorem 2.2 the threshold value in the case of Gaussian distribution with mean  $\mu = 0$  and deviation 0.2 is

$$\hat{K}_c = 2 \left[ \int_{-\infty}^{\infty} \frac{\frac{\sigma^2}{2}}{\frac{\sigma^4}{4} + \omega'^2} g(\omega') d\omega' \right]^{-1} = 0.385422.$$

In the case of no noise we had  $K_c = 0.319154$ , therefore we can immediately observe that the phase transition, when there is noise, takes place *after*, i.e. for a larger value of  $K$ . Then we can note, in the figure 2.4, that for the first values of  $K$  we have  $r \approx 0$ , then, near the critical point  $\hat{K}_c$ ,  $r$  begins to increase and getting closer to 1. Therefore, at  $K \approx \hat{K}_c$  the phase transition occurs and the oscillators begin to synchronize. Also in this figure, it is visible the difference between the two cases: for  $K = 0.8$  the value of  $r$  is smaller than the corresponding value of  $r$  when there is no noise. In the

case of noise, we can also note, that for  $K = 1.2$  we have a value of  $r$  which is smaller than the value of  $r$  for  $K = 0.8$  in case of absence of noise. With greater values of number of oscillators and  $t_{\text{final}}$  the graphs are even better and more similar to the theoretical graph, figure 1.3.

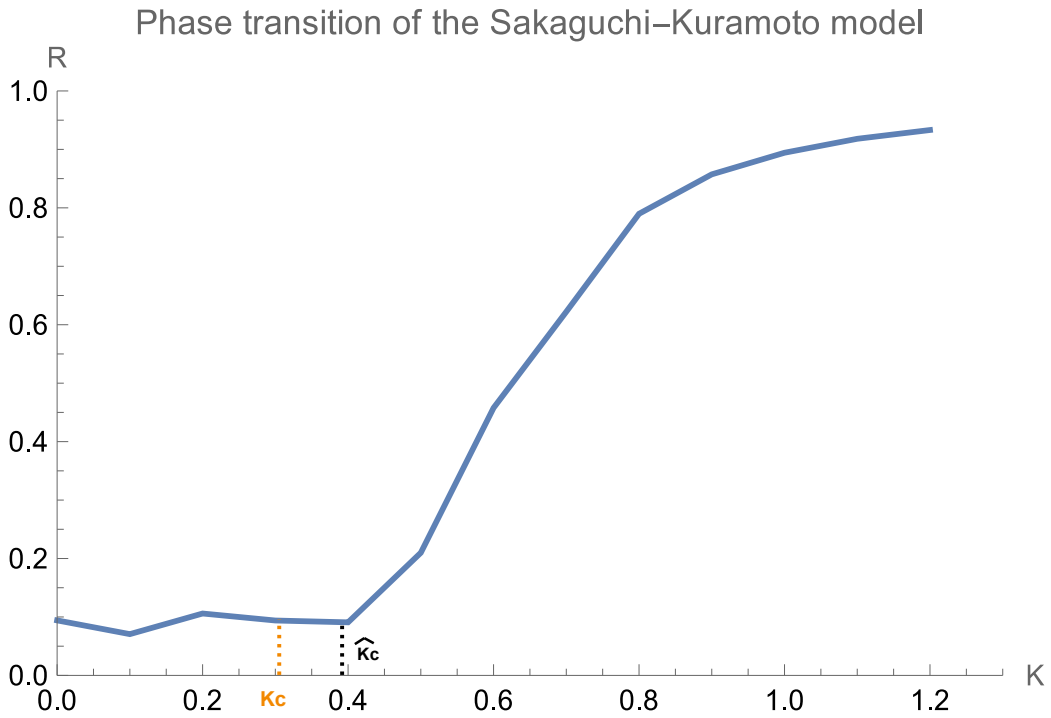


Figure 2.4: At  $K \approx 0.4$  the phase transition occurs, for  $K < \hat{K}_c$  the oscillators run incoherently, for  $K > \hat{K}_c$  they start to synchronize. For  $K = 0.8$  we have  $r \approx 0.8$ , instead for the same value of  $K$ , in the case of no noise we had  $r \approx 0.9$ . In the figure it is marked also the threshold value in absence of noise (in orange).

# Conclusions

The phenomenon of synchronization is a common event in everyday life and it is important to know how it works, how the various *entities* synchronize if originally they *run* independently. In this thesis we have studied the Kuramoto model which deals with the synchronization of a population of coupled limit-cycle oscillators. First we have analyzed the simple case without noise. We have transformed the original governing equations according to the mean-field theory, in order to make the treatment less difficult. Then, we have introduced the complex order parameter which is a macroscopic quantity which describes the synchronization behavior of the oscillators and it allows to represent the oscillators on the unit circle in the complex plane. It is useful to be able to represent the oscillators in order to visualize better their behavior. Analyzing the equations of the model and the solutions, we have found out that the synchronization between oscillators depends, above all, on the coupling strength constant  $K$ , that appears in the equations. As the coupling constant increases, the phenomenon of synchronization starts to come out, as we can see in the numerical simulations, and finally the oscillators run like a single oscillator. We have found the critical point of  $K$  at which the oscillators begin to synchronize that is the point at which the phase transition occurs. In fact if the value of  $K$  is very small,  $K \approx 0$ , the oscillators are not synchronized and they run independently, instead when the value of  $K$  exceeds the threshold value  $K_c$  the synchronization starts. The value of the coupling strength affects the value of the complex order parameter: the case  $r \approx 0$  means that the oscillators are completely incoherent, instead the opposite case  $r \approx 1$  tell us that they are synchronized. Finding the threshold value of  $K$  we have discovered that it depends only on the distribution of the natural frequencies that we have taken into account. Then we have studied the stability properties of the incoherent solution  $r = 0$  finding out that is neutrally stable for  $K \leq K_c$  and unstable for  $K > K_c$ . Finally we have considered the Kuramoto model with the presence of noise. There are some differences from the previous model. First of all the critical value depends also, as can be expected, on the strength of noise, then the

stability properties of the incoherent solution are not the same: for  $K < \hat{K}_c$  the incoherent solution can be also linearly stable. Finally, through the simulations, we have found out that if we consider the two models with the same assumptions (the natural frequencies are distributed according to the same probability distribution, the number of oscillators is the same and so on), if the coupling strength is the same the oscillators with noise are less synchronized than the noiseless one. When there is noise, the oscillators require a larger value of  $K$  to have the *same behavior* of the oscillators in case of no noise.



# Appendix A

## Mathematica codes

Here there is my Mathematica code that describes the Kuramoto model when there is no noise.

```
1 tfinal = 4000;
2
3 n = 250;
4
5 \[omega]= RandomVariate[NormalDistribution[0, 0.2], n];
6
7 kc = 2/(\[Pi] PDF[NormalDistribution[0, 0.2], 0])
8
9 \[Theta]0 = Mod[RandomVariate[NormalDistribution[0, 0.2], n],
10                2 \[Pi]];
11
12 (* Differential equations of the Kuramoto model *)
13
14 kuramotoODE0 = Table[\[Theta][i]'[t] == \[Omega][[i]]
15                    +(0/n)Sum[Sin[\[Theta][j][t]-\[Theta][i][t]],
16                    {j, 1, n}], {i, 1, n}];
17 kuramotoODE1 = Table[\[Theta][i]'[t] == \[Omega][[i]]
18                    +(0.1/n)Sum[Sin[\[Theta][j][t]-\[Theta][i][t]],
19                    {j, 1, n}], {i, 1, n}];
20 kuramotoODE2 = Table[\[Theta][i]'[t] == \[Omega][[i]]
21                    +(0.2/n)Sum[Sin[\[Theta][j][t]-\[Theta][i][t]],
22                    {j, 1, n}], {i, 1, n}];
23 kuramotoODE3 = Table[\[Theta][i]'[t] == \[Omega][[i]]
24                    +(0.3/n)Sum[Sin[\[Theta][j][t]-\[Theta][i][t]],
25                    {j, 1, n}], {i, 1, n}];
26 kuramotoODE4 = Table[\[Theta][i]'[t] == \[Omega][[i]]
27                    +(0.4/n)Sum[Sin[\[Theta][j][t]-\[Theta][i][t]],
28                    {j, 1, n}], {i, 1, n}];
29 kuramotoODE5 = Table[\[Theta][i]'[t] == \[Omega][[i]]
30                    +(0.5/n)Sum[Sin[\[Theta][j][t]-\[Theta][i][t]],
```

```

31      {j, 1, n} , {i, 1, n}];
32 kuramotoODE6 = Table[\[Theta][i]'[t] == \[Omega][[i]]
33      +(0.6/n)Sum[Sin[\[Theta][j][t]-\[Theta][i][t]],
34      {j, 1, n} , {i, 1, n}];
35 kuramotoODE7 = Table[\[Theta][i]'[t] == \[Omega][[i]]
36      +(0.7/n)Sum[Sin[\[Theta][j][t]-\[Theta][i][t]],
37      {j, 1, n} , {i, 1, n}];
38 kuramotoODE8 = Table[\[Theta][i]'[t] == \[Omega][[i]]
39      +(0.8/n)Sum[Sin[\[Theta][j][t]-\[Theta][i][t]],
40      {j, 1, n} , {i, 1, n}];
41
42 (* Initial conditions *)
43
44 initialConditions = Table[\[Theta][i][0] == \[Theta]0[[i]],
45      {i, 1, n}];
46
47 (* Solutions *)
48
49 sol0 = NDSolve[{kuramotoODE0, initialConditions},
50      Table[\[Theta][i], {i, 1, n}], {t, 0, tfinal}];
51 sol1 = NDSolve[{kuramotoODE1, initialConditions},
52      Table[\[Theta][i], {i, 1, n}], {t, 0, tfinal}];
53 sol2 = NDSolve[{kuramotoODE2, initialConditions},
54      Table[\[Theta][i], {i, 1, n}], {t, 0, tfinal}];
55 sol3 = NDSolve[{kuramotoODE3, initialConditions},
56      Table[\[Theta][i], {i, 1, n}], {t, 0, tfinal}];
57 sol4 = NDSolve[{kuramotoODE4, initialConditions},
58      Table[\[Theta][i], {i, 1, n}], {t, 0, tfinal}];
59 sol5 = NDSolve[{kuramotoODE5, initialConditions},
60      Table[\[Theta][i], {i, 1, n}], {t, 0, tfinal}];
61 sol6 = NDSolve[{kuramotoODE6, initialConditions},
62      Table[\[Theta][i], {i, 1, n}], {t, 0, tfinal}];
63 sol7 = NDSolve[{kuramotoODE7, initialConditions},
64      Table[\[Theta][i], {i, 1, n}], {t, 0, tfinal}];
65 sol8 = NDSolve[{kuramotoODE8, initialConditions},
66      Table[\[Theta][i], {i, 1, n}], {t, 0, tfinal}];
67
68
69
70 (* Order parameter *)
71
72 R[t_] := Abs[1/n Sum[Exp[I \[Theta][i][t] ], {i, 1, n}]];
73 R0 = R[tfinal] /. sol0[[1]];
74 R1 = R[tfinal] /. sol1[[1]];
75 R2 = R[tfinal] /. sol2[[1]];
76 R3 = R[tfinal] /. sol3[[1]];
77 R4 = R[tfinal] /. sol4[[1]];
78 R5 = R[tfinal] /. sol5[[1]];
79 R6 = R[tfinal] /. sol6[[1]];

```

```

80 R7 = R[tfinal] /. sol7[[1]];
81 R8 = R[tfinal] /. sol8[[1]];
82
83
84
85 (* Lists of solutions *)
86
87 l0 = Table[\[Theta][i][tfinal], {i, 1, n}] /. sol0[[1]];
88 l1 = Table[\[Theta][i][tfinal], {i, 1, n}] /. sol1[[1]];
89 l2 = Table[\[Theta][i][tfinal], {i, 1, n}] /. sol2[[1]];
90 l3 = Table[\[Theta][i][tfinal], {i, 1, n}] /. sol3[[1]];
91 l4 = Table[\[Theta][i][tfinal], {i, 1, n}] /. sol4[[1]];
92 l5 = Table[\[Theta][i][tfinal], {i, 1, n}] /. sol5[[1]];
93 l6 = Table[\[Theta][i][tfinal], {i, 1, n}] /. sol6[[1]];
94 l7 = Table[\[Theta][i][tfinal], {i, 1, n}] /. sol7[[1]];
95 l8 = Table[\[Theta][i][tfinal], {i, 1, n}] /. sol8[[1]];
96
97 (* Centroids of phases *)
98
99 p0 = Mean@Table[{Cos[phase], Sin[phase]}, {phase, l0}];
100 p1 = Mean@Table[{Cos[phase], Sin[phase]}, {phase, l1}];
101 p2 = Mean@Table[{Cos[phase], Sin[phase]}, {phase, l2}];
102 p3 = Mean@Table[{Cos[phase], Sin[phase]}, {phase, l3}];
103 p4 = Mean@Table[{Cos[phase], Sin[phase]}, {phase, l4}];
104 p5 = Mean@Table[{Cos[phase], Sin[phase]}, {phase, l5}];
105 p6 = Mean@Table[{Cos[phase], Sin[phase]}, {phase, l6}];
106 p7 = Mean@Table[{Cos[phase], Sin[phase]}, {phase, l7}];
107 p8 = Mean@Table[{Cos[phase], Sin[phase]}, {phase, l8}];
108
109 (* Plot phase transition*)
110
111 ListPlot[{{0,R0}, {0.1,R1}, {0.2,R2}, {0.3,R3}, {0.4,R4},
112          {0.5,R5}, {0.6,R6}, {0.7,R7}, {0.8,R8}},
113          AxesLabel -> {"K", "R"},
114          PlotRange -> {{0, 1}, {0, 1}}, Joined -> True,
115          PlotLabel -> "Phase transition of the Kuramoto model"
116          ]
117
118 (*Plot unit circle *)
119
120 Graphics[{Circle[], PointSize[0.03],
121           Point[Table[{Cos[phase], Sin[phase]}, {phase, l0}]],
122           Thickness[0.01], Orange, Arrowheads[0.07], Arrow[{{0, 0},
123           p0}]],
124           AspectRatio -> 1, PlotRange -> {{-1.1, 1.1}, {-1.1, 1.1}},
125           ImageSize -> Small, PlotLabel -> K == 0]
126

```

```

127 Graphics[{Circle[], PointSize[0.03],
128   Point[Table[{Cos[phase], Sin[phase]}, {phase, 11}]],
129   Thickness[0.01], Orange, Arrowheads[0.07], Arrow[{{0, 0},
130     p1}}],
131   AspectRatio -> 1, PlotRange -> {{-1.1, 1.1}, {-1.1, 1.1}},
132   ImageSize -> Small, PlotLabel -> K == 0.1]
133
133 Graphics[{Circle[], PointSize[0.03],
134   Point[Table[{Cos[phase], Sin[phase]}, {phase, 12}]],
135   Thickness[0.01], Orange, Arrowheads[0.07], Arrow[{{0, 0},
136     p2}}],
137   AspectRatio -> 1, PlotRange -> {{-1.1, 1.1}, {-1.1, 1.1}},
138   ImageSize -> Small, PlotLabel -> K == 0.2]
139
139 Graphics[{Circle[], PointSize[0.03],
140   Point[Table[{Cos[phase], Sin[phase]}, {phase, 13}]],
141   Thickness[0.01], Orange, Arrowheads[0.07], Arrow[{{0, 0},
142     p3}}],
143   AspectRatio -> 1, PlotRange -> {{-1.1, 1.1}, {-1.1, 1.1}},
144   ImageSize -> Small, PlotLabel -> K == 0.3]
145
145 Graphics[{Circle[], PointSize[0.03],
146   Point[Table[{Cos[phase], Sin[phase]}, {phase, 14}]],
147   Thickness[0.01], Orange, Arrowheads[0.07], Arrow[{{0, 0},
148     p4}}],
149   AspectRatio -> 1, PlotRange -> {{-1.1, 1.1}, {-1.1, 1.1}},
150   ImageSize -> Small, PlotLabel -> K == 0.4]
151
151 Graphics[{Circle[], PointSize[0.03],
152   Point[Table[{Cos[phase], Sin[phase]}, {phase, 15}]],
153   Thickness[0.01], Orange, Arrowheads[0.07], Arrow[{{0, 0},
154     p5}}],
155   AspectRatio -> 1, PlotRange -> {{-1.1, 1.1}, {-1.1, 1.1}},
156   ImageSize -> Small, PlotLabel -> K == 0.5]
157
157 Graphics[{Circle[], PointSize[0.03],
158   Point[Table[{Cos[phase], Sin[phase]}, {phase, 16}]],
159   Thickness[0.01], Orange, Arrowheads[0.07], Arrow[{{0, 0},
160     p6}}],
161   AspectRatio -> 1, PlotRange -> {{-1.1, 1.1}, {-1.1, 1.1}},
162   ImageSize -> Small, PlotLabel -> K == 0.6]
163
163 Graphics[{Circle[], PointSize[0.03],
164   Point[Table[{Cos[phase], Sin[phase]}, {phase, 17}]],
165   Thickness[0.01], Orange, Arrowheads[0.07], Arrow[{{0, 0},
166     p7}}],
167   AspectRatio -> 1, PlotRange -> {{-1.1, 1.1}, {-1.1, 1.1}},
168   ImageSize -> Small, PlotLabel -> K == 0.7]

```

```

169 Graphics[{Circle[], PointSize[0.03],
170   Point[Table[{Cos[phase], Sin[phase]}, {phase, 18}]],
171   Thickness[0.01], Orange, Arrowheads[0.07], Arrow[{{0, 0},
    p8}]],
172 AspectRatio -> 1, PlotRange -> {{-1.1, 1.1}, {-1.1, 1.1}},
173 ImageSize -> Small, PlotLabel -> K == 0.8]

```

Here, there is the Mathematica code that describes the Sakaguchi-Kuramoto model. I call  $\beta$  the term  $\sigma^2$  of the noise strength to not confuse it with the deviation of the Gaussian distribution.

```

1 tfinal = 4000;
2
3 dt = 1;
4
5 \[Beta] = 0.1;
6
7 n = 250;
8
9 \[Omega] = RandomVariate[NormalDistribution[0, 0.2], n];
10
11 kc = 2(Integrate[(\[Beta]/2)PDF[NormalDistribution[0, 0.2],x
    ]/((\[Beta]^2/4) + x^2), {x, -Infinity, +Infinity}])^(-1)
12
13 \[Theta]0 = Mod[RandomVariate[NormalDistribution[0, 0.2], n],
    2\[Pi]];
14
15 X = RandomVariate[NormalDistribution[0, 1], n];
16
17 (* Differential equations of the Sakaguchi-Kuramoto model*)
18 kuramotoODE0 = Table[\[Theta][i]'[t]==Sqrt[\[Beta]](1/Sqrt[dt
    ])X[[i]]+\[Omega][[i]]+(0/n)Sum[Sin[\[Theta][j][t]-\[Theta
    ][i][t]],{j, 1, n}],{i, 1, n}];
19 kuramotoODE1 = Table[\[Theta][i]'[t]==Sqrt[\[Beta]](1/Sqrt[dt
    ])X[[i]]+\[Omega][[i]]+(0.1/n)Sum[Sin[\[Theta][j][t]-\[
    Theta][i][t]],{j, 1, n}],{i, 1, n}];
20 kuramotoODE2 = Table[\[Theta][i]'[t]==Sqrt[\[Beta]](1/Sqrt[dt
    ])X[[i]]+\[Omega][[i]]+(0.2/n)Sum[Sin[\[Theta][j][t]-\[
    Theta][i][t]],{j, 1, n}],{i, 1, n}];
21 kuramotoODE3 = Table[\[Theta][i]'[t]==Sqrt[\[Beta]](1/Sqrt[dt
    ])X[[i]]+\[Omega][[i]]+(0.3/n)Sum[Sin[\[Theta][j][t]-\[
    Theta][i][t]],{j, 1, n}],{i, 1, n}];
22 kuramotoODE4 = Table[\[Theta][i]'[t]==Sqrt[\[Beta]](1/Sqrt[dt
    ])X[[i]]+\[Omega][[i]]+(0.4/n)Sum[Sin[\[Theta][j][t]-\[
    Theta][i][t]],{j, 1, n}],{i, 1, n}];
23 kuramotoODE5 = Table[\[Theta][i]'[t]==Sqrt[\[Beta]](1/Sqrt[dt
    ])X[[i]]+\[Omega][[i]]+(0.5/n)Sum[Sin[\[Theta][j][t]-\[
    Theta][i][t]],{j, 1, n}],{i, 1, n}];

```

```

24 kuramotoODE6 = Table[\[Theta][i]'[t]==Sqrt[\[Beta]](1/Sqrt[dt
    ])X[[i]]+\[Omega][[i]]+(0.6/n)Sum[Sin[\[Theta][j][t]-\[
    Theta][i][t]],{j, 1, n}],{i, 1, n}];
25 kuramotoODE7 = Table[\[Theta][i]'[t]==Sqrt[\[Beta]](1/Sqrt[dt
    ])X[[i]]+\[Omega][[i]]+(0.7/n)Sum[Sin[\[Theta][j][t]-\[
    Theta][i][t]],{j, 1, n}],{i, 1, n}];
26 kuramotoODE8 = Table[\[Theta][i]'[t]==Sqrt[\[Beta]](1/Sqrt[dt
    ])X[[i]]+\[Omega][[i]]+(0.8/n)Sum[Sin[\[Theta][j][t]-\[
    Theta][i][t]],{j, 1, n}],{i, 1, n}];
27 kuramotoODE9 = Table[\[Theta][i]'[t]==Sqrt[\[Beta]](1/Sqrt[dt
    ])X[[i]]+\[Omega][[i]]+(0.9/n)Sum[Sin[\[Theta][j][t]-\[
    Theta][i][t]],{j, 1, n}],{i, 1, n}];
28 kuramotoODE10 = Table[\[Theta][i]'[t]==Sqrt[\[Beta]](1/Sqrt[
    dt])X[[i]]+\[Omega][[i]]+(1/n)Sum[Sin[\[Theta][j][t]-\[
    Theta][i][t]],{j, 1, n}],{i, 1, n}];
29 kuramotoODE11 = Table[\[Theta][i]'[t]==Sqrt[\[Beta]](1/Sqrt[
    dt])X[[i]]+\[Omega][[i]]+(1.1/n)Sum[Sin[\[Theta][j][t]-\[
    Theta][i][t]],{j, 1, n}],{i, 1, n}];
30 kuramotoODE12 = Table[\[Theta][i]'[t]==Sqrt[\[Beta]](1/Sqrt[
    dt])X[[i]]+\[Omega][[i]]+(1.2/n)Sum[Sin[\[Theta][j][t]-\[
    Theta][i][t]],{j, 1, n}],{i, 1, n}];
31
32
33 (* Initial conditions *)
34 initialConditions = Table[\[Theta][i][0] == \[Theta]0[[i]], {
    i, 1, n}];
35
36 (* Solutions *)
37 sol0 = NDSolve[{kuramotoODE0, initialConditions},
38   Table[\[Theta][i], {i, 1, n}], {t, 0, tfinal}];
39 sol1 = NDSolve[{kuramotoODE1, initialConditions},
40   Table[\[Theta][i], {i, 1, n}], {t, 0, tfinal}];
41 sol2 = NDSolve[{kuramotoODE2, initialConditions},
42   Table[\[Theta][i], {i, 1, n}], {t, 0, tfinal}];
43 sol3 = NDSolve[{kuramotoODE3, initialConditions},
44   Table[\[Theta][i], {i, 1, n}], {t, 0, tfinal}];
45 sol4 = NDSolve[{kuramotoODE4, initialConditions},
46   Table[\[Theta][i], {i, 1, n}], {t, 0, tfinal}];
47 sol5 = NDSolve[{kuramotoODE5, initialConditions},
48   Table[\[Theta][i], {i, 1, n}], {t, 0, tfinal}];
49 sol6 = NDSolve[{kuramotoODE6, initialConditions},
50   Table[\[Theta][i], {i, 1, n}], {t, 0, tfinal}];
51 sol7 = NDSolve[{kuramotoODE7, initialConditions},
52   Table[\[Theta][i], {i, 1, n}], {t, 0, tfinal}];
53 sol8 = NDSolve[{kuramotoODE8, initialConditions},
54   Table[\[Theta][i], {i, 1, n}], {t, 0, tfinal}];
55 sol9 = NDSolve[{kuramotoODE9, initialConditions},
56   Table[\[Theta][i], {i, 1, n}], {t, 0, tfinal}];
57 sol10 = NDSolve[{kuramotoODE10, initialConditions},

```

```

58 Table[\[Theta][i], {i, 1, n}], {t, 0, tfinal}];
59 sol11 = NDSolve[{kuramotoODE11, initialConditions},
60 Table[\[Theta][i], {i, 1, n}], {t, 0, tfinal}];
61 sol12 = NDSolve[{kuramotoODE12, initialConditions},
62 Table[\[Theta][i], {i, 1, n}], {t, 0, tfinal}];
63 (* Order parameter *)
64 R[t_] := Abs[1/n Sum[Exp[I \[Theta][i][t] ], {i, 1, n}]];
65 R0 = R[tfinal] /. sol10[[1]];
66 R1 = R[tfinal] /. sol11[[1]];
67 R2 = R[tfinal] /. sol12[[1]];
68 R3 = R[tfinal] /. sol13[[1]];
69 R4 = R[tfinal] /. sol14[[1]];
70 R5 = R[tfinal] /. sol15[[1]];
71 R6 = R[tfinal] /. sol16[[1]];
72 R7 = R[tfinal] /. sol17[[1]];
73 R8 = R[tfinal] /. sol18[[1]];
74 R9 = R[tfinal] /. sol19[[1]];
75 R10 = R[tfinal] /. sol10[[1]];
76 R11 = R[tfinal] /. sol11[[1]];
77 R12 = R[tfinal] /. sol12[[1]];
78
79 (* Lists of solutions *)
80 l0 = Table[\[Theta][i][tfinal], {i, 1, n} /. sol10[[1]];
81 l1 = Table[\[Theta][i][tfinal], {i, 1, n} /. sol11[[1]];
82 l2 = Table[\[Theta][i][tfinal], {i, 1, n} /. sol12[[1]];
83 l3 = Table[\[Theta][i][tfinal], {i, 1, n} /. sol13[[1]];
84 l4 = Table[\[Theta][i][tfinal], {i, 1, n} /. sol14[[1]];
85 l5 = Table[\[Theta][i][tfinal], {i, 1, n} /. sol15[[1]];
86 l6 = Table[\[Theta][i][tfinal], {i, 1, n} /. sol16[[1]];
87 l7 = Table[\[Theta][i][tfinal], {i, 1, n} /. sol17[[1]];
88 l8 = Table[\[Theta][i][tfinal], {i, 1, n} /. sol18[[1]];
89 l9 = Table[\[Theta][i][tfinal], {i, 1, n} /. sol19[[1]];
90 l10 = Table[\[Theta][i][tfinal], {i, 1, n} /. sol10[[1]];
91 l11 = Table[\[Theta][i][tfinal], {i, 1, n} /. sol11[[1]];
92 l12 = Table[\[Theta][i][tfinal], {i, 1, n} /. sol12[[1]];
93
94 (* Centroids of phases *)
95 p0 = Mean@Table[{Cos[phase], Sin[phase]}, {phase, 10}];
96 p1 = Mean@Table[{Cos[phase], Sin[phase]}, {phase, 11}];
97 p2 = Mean@Table[{Cos[phase], Sin[phase]}, {phase, 12}];
98 p3 = Mean@Table[{Cos[phase], Sin[phase]}, {phase, 13}];
99 p4 = Mean@Table[{Cos[phase], Sin[phase]}, {phase, 14}];
100 p5 = Mean@Table[{Cos[phase], Sin[phase]}, {phase, 15}];
101 p6 = Mean@Table[{Cos[phase], Sin[phase]}, {phase, 16}];
102 p7 = Mean@Table[{Cos[phase], Sin[phase]}, {phase, 17}];
103 p8 = Mean@Table[{Cos[phase], Sin[phase]}, {phase, 18}];
104 p9 = Mean@Table[{Cos[phase], Sin[phase]}, {phase, 19}];
105 p10 = Mean@Table[{Cos[phase], Sin[phase]}, {phase, 110}];
106 p11 = Mean@Table[{Cos[phase], Sin[phase]}, {phase, 111}];

```

```

107 p12 = Mean@Table[{Cos[phase], Sin[phase]}, {phase, 112}];
108
109 (* Plot phase transition*)
110 ListPlot[{{0, R0}, {0.1, R1}, {0.2, R2}, {0.3, R3}, {0.4, R4
111 }, {0.5,
112 R5}, {0.6, R6}, {0.7, R7}, {0.8, R8}, {0.9, R9}, {1, R10},
113 {1.1,
114 R11}, {1.2, R12}}, AxesLabel -> {"K", "R"},
115 PlotRange -> {{0, 1.3}, {0, 1}}, Joined -> True,
116 PlotLabel -> "Phase transition of the Sakaguchi-Kuramoto
117 model"]
118
119 (*Plot unit circle *)
120 Graphics[{Circle[], PointSize[0.03],
121 Point[Table[{Cos[phase], Sin[phase]}, {phase, 10}]],
122 Thickness[0.01], Orange, Arrowheads[0.07], Arrow[{{0, 0},
123 p0}]],
124 AspectRatio -> 1, PlotRange -> {{-1.1, 1.1}, {-1.1, 1.1}},
125 ImageSize -> Small, PlotLabel -> K == 0]
126 Graphics[{Circle[], PointSize[0.03],
127 Point[Table[{Cos[phase], Sin[phase]}, {phase, 11}]],
128 Thickness[0.01], Orange, Arrowheads[0.07], Arrow[{{0, 0},
129 p1}]],
130 AspectRatio -> 1, PlotRange -> {{-1.1, 1.1}, {-1.1, 1.1}},
131 ImageSize -> Small, PlotLabel -> K == 0.1]
132 Graphics[{Circle[], PointSize[0.03],
133 Point[Table[{Cos[phase], Sin[phase]}, {phase, 12}]],
134 Thickness[0.01], Orange, Arrowheads[0.07], Arrow[{{0, 0},
135 p2}]],
136 AspectRatio -> 1, PlotRange -> {{-1.1, 1.1}, {-1.1, 1.1}},
137 ImageSize -> Small, PlotLabel -> K == 0.2]
138 Graphics[{Circle[], PointSize[0.03],
139 Point[Table[{Cos[phase], Sin[phase]}, {phase, 13}]],
140 Thickness[0.01], Orange, Arrowheads[0.07], Arrow[{{0, 0},
141 p3}]],
142 AspectRatio -> 1, PlotRange -> {{-1.1, 1.1}, {-1.1, 1.1}},
143 ImageSize -> Small, PlotLabel -> K == 0.3]
144 Graphics[{Circle[], PointSize[0.03],
145 Point[Table[{Cos[phase], Sin[phase]}, {phase, 14}]],
146 Thickness[0.01], Orange, Arrowheads[0.07], Arrow[{{0, 0},
147 p4}]],
148 AspectRatio -> 1, PlotRange -> {{-1.1, 1.1}, {-1.1, 1.1}},
149 ImageSize -> Small, PlotLabel -> K == 0.4]
150 Graphics[{Circle[], PointSize[0.03],
151 Point[Table[{Cos[phase], Sin[phase]}, {phase, 15}]],
152 Thickness[0.01], Orange, Arrowheads[0.07], Arrow[{{0, 0},
153 p5}]],
154 AspectRatio -> 1, PlotRange -> {{-1.1, 1.1}, {-1.1, 1.1}},
155 ImageSize -> Small, PlotLabel -> K == 0.5]

```



```

147 Graphics [{Circle[], PointSize[0.03],
148   Point[Table[{Cos[phase], Sin[phase]}, {phase, 16}]],
149   Thickness[0.01], Orange, Arrowheads[0.07], Arrow[{{0, 0},
    p6}]],
150 AspectRatio -> 1, PlotRange -> {{-1.1, 1.1}, {-1.1, 1.1}},
151 ImageSize -> Small, PlotLabel -> K == 0.6]
152 Graphics [{Circle[], PointSize[0.03],
153   Point[Table[{Cos[phase], Sin[phase]}, {phase, 17}]],
154   Thickness[0.01], Orange, Arrowheads[0.07], Arrow[{{0, 0},
    p7}]],
155 AspectRatio -> 1, PlotRange -> {{-1.1, 1.1}, {-1.1, 1.1}},
156 ImageSize -> Small, PlotLabel -> K == 0.7]
157 Graphics [{Circle[], PointSize[0.03],
158   Point[Table[{Cos[phase], Sin[phase]}, {phase, 18}]],
159   Thickness[0.01], Orange, Arrowheads[0.07], Arrow[{{0, 0},
    p8}]],
160 AspectRatio -> 1, PlotRange -> {{-1.1, 1.1}, {-1.1, 1.1}},
161 ImageSize -> Small, PlotLabel -> K == 0.8]
162 Graphics[{Circle[], PointSize[0.03],
163   Point[Table[{Cos[phase], Sin[phase]}, {phase, 19}]],
164   Thickness[0.01], Orange, Arrowheads[0.07], Arrow[{{0, 0},
    p9}]],
165 AspectRatio -> 1, PlotRange -> {{-1.1, 1.1}, {-1.1, 1.1}},
166 ImageSize -> Small, PlotLabel -> K == 0.9]
167 Graphics[{Circle[], PointSize[0.03],
168   Point[Table[{Cos[phase], Sin[phase]}, {phase, 110}]],
169   Thickness[0.01], Orange, Arrowheads[0.07], Arrow[{{0, 0},
    p10}]],
170 AspectRatio -> 1, PlotRange -> {{-1.1, 1.1}, {-1.1, 1.1}},
171 ImageSize -> Small, PlotLabel -> K == 1]
172 Graphics[{Circle[], PointSize[0.03],
173   Point[Table[{Cos[phase], Sin[phase]}, {phase, 111}]],
174   Thickness[0.01], Orange, Arrowheads[0.07], Arrow[{{0, 0},
    p11}]],
175 AspectRatio -> 1, PlotRange -> {{-1.1, 1.1}, {-1.1, 1.1}},
176 ImageSize -> Small, PlotLabel -> K == 1.1]
177 Graphics[{Circle[], PointSize[0.03],
178   Point[Table[{Cos[phase], Sin[phase]}, {phase, 112}]],
179   Thickness[0.01], Orange, Arrowheads[0.07], Arrow[{{0, 0},
    p12}]],
180 AspectRatio -> 1, PlotRange -> {{-1.1, 1.1}, {-1.1, 1.1}},
181 ImageSize -> Small, PlotLabel -> K == 1.2]

```



# Bibliography

- [1] S. H. Strogatz. *From Kuramoto to Crawford: exploring the onset of synchronization in populations of coupled oscillators*, Physica D 143 p.10 (2000).
- [2] A. Pikovsky, M. Rosenblum and J. Kurths. *Synchronization, a universal concept in nonlinear sciences*, Appendix A1, Cambridge Nonlinear Science Series 12 (2001).
- [3] J. G. Restrepo, E. Ott, B. R. Hunt. *Synchronization in large directed networks of coupled phase oscillators*, Chaos 16 (2006).
- [4] R. E. Mirollo and S. H. Strogatz. *Stability of Incoherence in a Population of Coupled Oscillators*, J. Statist. Phys. 63 (1991).
- [5] R. E. Mirollo and S. H. Strogatz. *Amplitude Death in an Array of Limit-Cycle Oscillators*, J. Statist. Phys. 60 (1990).
- [6] P. Baldi. *Stochastic Calculus*, Springer (2017).